International Journal of Geoheritage and Parks 13 (2025) 616–637

Contents lists available at ScienceDirect

International Journal of Geoheritage and Parks

journal homepage: http://www.keaipublishing.com/en/journals/international-journal-of-geoheritage-and-parks/

Research Paper

Geomorphological perspective of geodiversity: A case study of Al–Zubaidat area, east of Misan Governorate (Iraq)

Bashar F. Maaroof [a,*], Hashim H. Kareem [b], Ban Al-Hasani [c], Iacopo Carnacina [c], Mawada Abdellatif [c], Nadhir Al-Ansari [d], Rayan G. Thannoun [e], Jaffar H. Al-Zubaydi [f], Varoujan K. Sissakian [g], Mohammed A. Al-Musawi [h], Raheem H. Al-Abdan [i], Jaafar Jotheri [j,k], Hussain M. Hussain [l], Manal Sh. Al-Kubaisi [m], Ahmed M. Hashoosh [n]

[a] Department of Geography, University of Babylon, Hillah, Babil 51001, Iraq
[b] Department of General Sciences, University of Misan, Amarah, Misan 62001, Iraq
[c] Civil Engineering and Built Environment Department, Faculty of Engineering Technology, Liverpool John Moores University, Liverpool L3 5UX, UK
[d] Department of Civil, Environmental, and Natural Resources Engineering, Lulea University of Technology, Lulea, 97187, Sweden
[e] Remote Sensing Center, University of Mosul, Mosul, AZ 6231, Iraq
[f] Department of Applied Geology, University of Babylon, Hillah, Babil 51001, Iraq
[g] Department of Earth Sciences, University of Kurdistan, Hewler, Erbil 44001, Iraq
[h] Department of Geography, University of Misan, Amarah, Misan, 62001, Iraq
[i] Department of Geography, University of Thi Qar, Al-Nasiriyah, Di Qar 64001, Iraq
[j] Department of Archaeology, University of Al-Qadisiya, Diwaniyah 58001, Iraq
[k] Department of Archaeology, Durham University, Durham DH1 3LE, UK
[l] Department of Geology, University of Kufa, Kufa 540011, Iraq
[m] Department of Geology, University of Baghdad, Baghdad 10001, Iraq
[n] Ministry of Water Resources, General Commission for Groundwater, Baghdad 10001, Iraq

ARTICLE INFO

Article history:
Received 16 July 2024
Received in revised form 3 November 2025
Accepted 13 November 2025

Available online 15 November 2025

Keywords:
geomorphology
geodiversity
geosite
geoheritage
AL–Zubaidat area

ABSTRACT

This research investigates the geodiversity of the AL-Zubaidat region in Southeastern Iraq, with a focus on its geomorphological and hydrological characteristics. This information helps researchers identify suitable locations for natural reserves, thereby enhancing the protection of Iraqi biodiversity. The region attracts eco-tourism visitors, benefiting the economy and providing various scientific, cultural, educational, and aesthetic benefits. This research employed the geoinformatics methodology for geospatial analysis, constructing a comprehensive geodatabase, categorizing spatial features through topographic, geological, and hydrological maps, and correlating data with satellite imagery and elevation models. Geodiversity was classified according to physical parameters and international criteria, with the final classification attributes formulated utilizing maps, field photographs, and geodatabases. The research employed specific parameters to analyze the geomorphometric and slope diversity of the Al-Zubaidat area watersheds. The study area in Al-Zubaidat comprises dome-shaped hills, tertiary geological formations, valleys, and badlands. The area encompasses 782.308 km^2 and shall consist of three principal watersheds (Al-Sharhani, Abu-Ghraibat, and Al-Shakak), as well as 12 sub-watersheds. The watershed perimeter is correlated with the circulating ratio, form factor, and elongation ratio, with larger perimeters generally indicating larger basin areas. The region encompasses low-slope terrain, with elevated slope values in the northern sections, especially in the headwaters. Geoheritage, geodiversity, geoconservation, and geoparks can facilitate sustainable development, promote healthy lifestyles, and foster cultural diversity. These initiatives

* Corresponding author.
E-mail address: basharma@uobabylon.edu.iq (B.F. Maaroof).

https://doi.org/10.1016/j.ijgeop.2025.11.002

are crucial for policymakers and regional stakeholders in semi-arid and developing regions, particularly in Southeast Asia, to enhance income and protect vulnerable natural resources.

1. Introduction

The notion of geodiversity first emerged in scientific literature during the 1990s. Ian Cray defines geodiversity as encompassing the natural spectrum of geological diversity (rocks, minerals, fossils), geomorphological diversity (landforms and physical processes), and soil properties (dispersal patterns and types) (Diniz, de Araújo, & das Chagas, 2022; Mucivuna, Garcia, Reynard, & Rosa, 2022; Najwer, Jankowski, Niesterowicz, & Zwoliński, 2022), including various types of water bodies and the physical processes that created them (Gordon, Crofts, Díaz-Martínez, & Woo, 2018; Kubalíková, 2020). Geodiversity denotes the variety of abiotic components within a specific area (Pardo-Igúzquiza & Dowd, 2021; L. S. Pereira & da Silva Farias, 2020). These elements constitute the landscape structure and, along with the biotic components, comprise the natural diversity of our planet (Henriques & Brilha, 2017).

Geodiversity stabilizes and sustains ecosystems (Quesada-Román & Pérez-Umaña, 2020). The geographical location of the ecosystem—whether it is situated in equatorial, tropical, or polar regions—influences the environmental quality of the landscape (Alexandrowicz & Margielewski, 2010; Gałaś et al., 2018; Gordon, Crofts, Gray, & Tormey, 2021). Since its inception, the notion of geodiversity has been linked to the terms "geography," "geoheritage," "geoconservation," "geopark," "geotourism," and "ecotourism" (Carrión-Mero, Montalván-Burbano, Herrera-Narváez, & Morante-Carballo, 2021; Gray, Gordon, & Brown, 2013; D. I. Pereira, Pereira, Brilha, & Santos, 2013). This concept has captivated earth scientists, geographers, and ecologists due to its scientific, educational, aesthetic, and cultural significance (Gordon, 2019).

Geodiversity enhances society and the natural environment by contributing to economic development, recreational pursuits, geotourism, and geoheritage (Carrión-Mero et al., 2021). It is crucial for biodiversity conservation as it offers a natural habitat for all organisms (Zarnetske et al., 2019). In contrast to biodiversity, the erroneous belief that geodiversity is inherently strong and resilient contributed to its lack of protection from collapse and degradation (Hjort, Heikkinen, & Luoto, 2012). Numerous studies have demonstrated that geodiversity is a non-renewable resource; its extent is finite and susceptible to both natural and anthropogenic threats. Recent evidence suggests that international agreements have addressed the issue of geodiversity in

Fig. 1. The study area is located in Southeastern Iraq.

a cursory manner (Mucivuna et al., 2022). Public policies have not prioritized safeguarding geodiversity, as demonstrated by national conservation agencies' absence of legal protective measures (Crofts, 2019).

The terrain of Iraq is characterized by its geodiversity, encompassing a wide range of geological formations, diverse geomorphological characteristics, varied soil compositions, and abundant water resources. This encourages researchers in earth science, geography, and environmental science to investigate geodiversity. Such studies can help identify optimal locations for natural reserves, thereby positively impacting the conservation of Iraqi biodiversity. The present study elucidates the AL-Zubaidat region in Southeastern Iraq, specifically within the Misan Governorate. The significance of the survey lies in its revelation of the geodiversity of the AL-Zubaidat area, encompassing geological, geomorphological, and pedological aspects. This facilitates a profound comprehension of the region's ecology, which may be designated as a reserve. They annually offer eco-tourism activities to tourists from both domestic and international locations, positively impacting the nation's economy. Furthermore, establishing the AL-Zubaidat area as a national reserve confers numerous scientific, cultural, educational, and aesthetic benefits.

The research problem can be defined as follows: Do physical geographical factors affect the formation and development of geodiversity in the Al-Zubaydat region? This study seeks to (a) examine the geodiversity, geoconservation, geomorphological, and hydrological diversity in the Al-Zubaydat region in Southeastern Iraq, and (b) delineate along with map the geodiversity of the Al-Zubaydat area, which includes river systems, hills, fault scarps, valleys, badlands, alluvial plains, alluvial fans, floodplains, meanders, and dunes on a regional scale.

2. Materials and methods

2.1. Study area

The Al-Zubaidat area is in the eastern section of Misan Governorate, Southeastern Iraq, within the East Tigris region (Maaroof, 2025). It is bordered north and northeast by Iranian territory; east, south, and southeast by Al-Sanaf Marsh, and west by the Al-Teeb River (Maaroof et al., 2023. The study area is situated between longitudes 47°09′2.489″E and 47°28′54.156″E and latitudes 32°5′50.932″N and 32°29′48.133″N, encompassing an area of 782.308 km^2. The study area is located in the eastern section of the Iraqi alluvial plain, distinguished by its floodplains and expansive marshes. Al-Sanaf Marsh, a prominent wetland situated south of the study area, receives water from the river drainage basins within the region, specifically Al-Sharhani, Abu Ghraibat, and

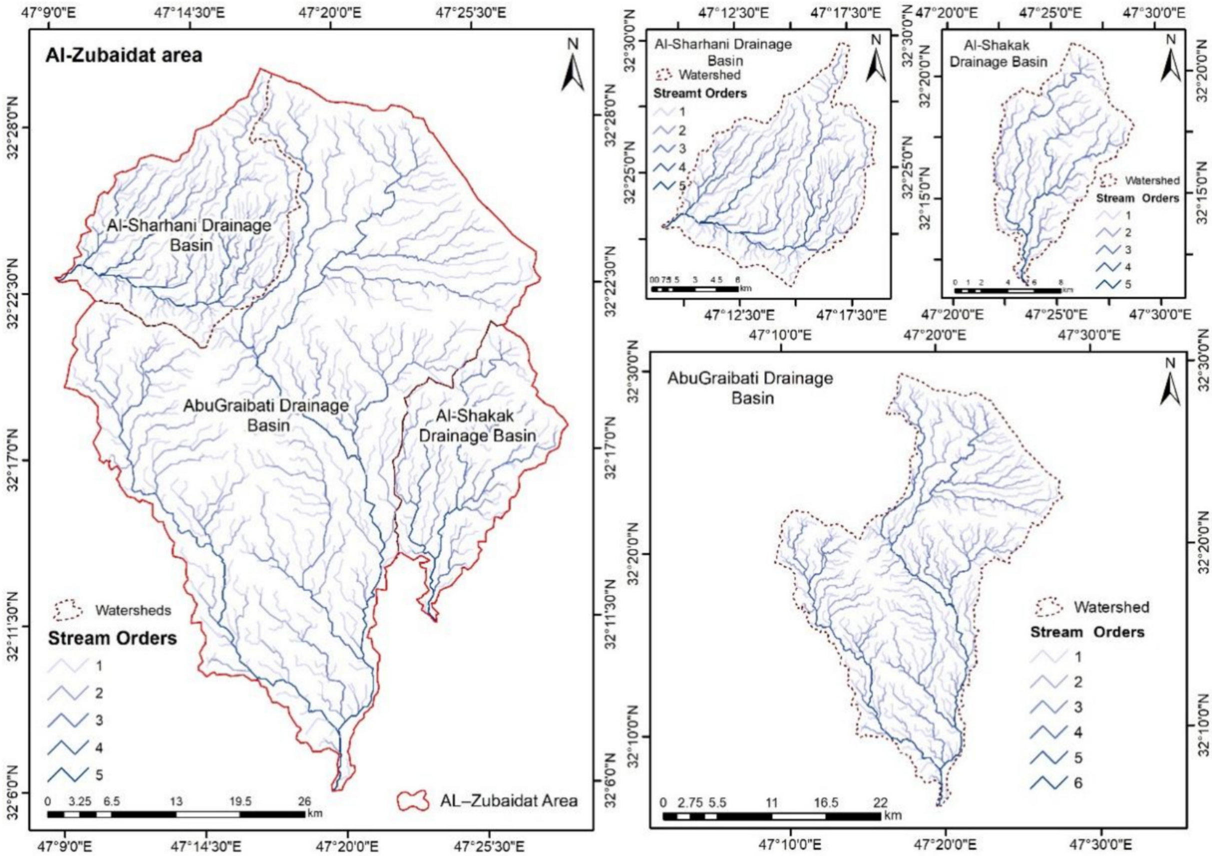

Fig. 2. River drainage basins of the Al-Zubaidat area.

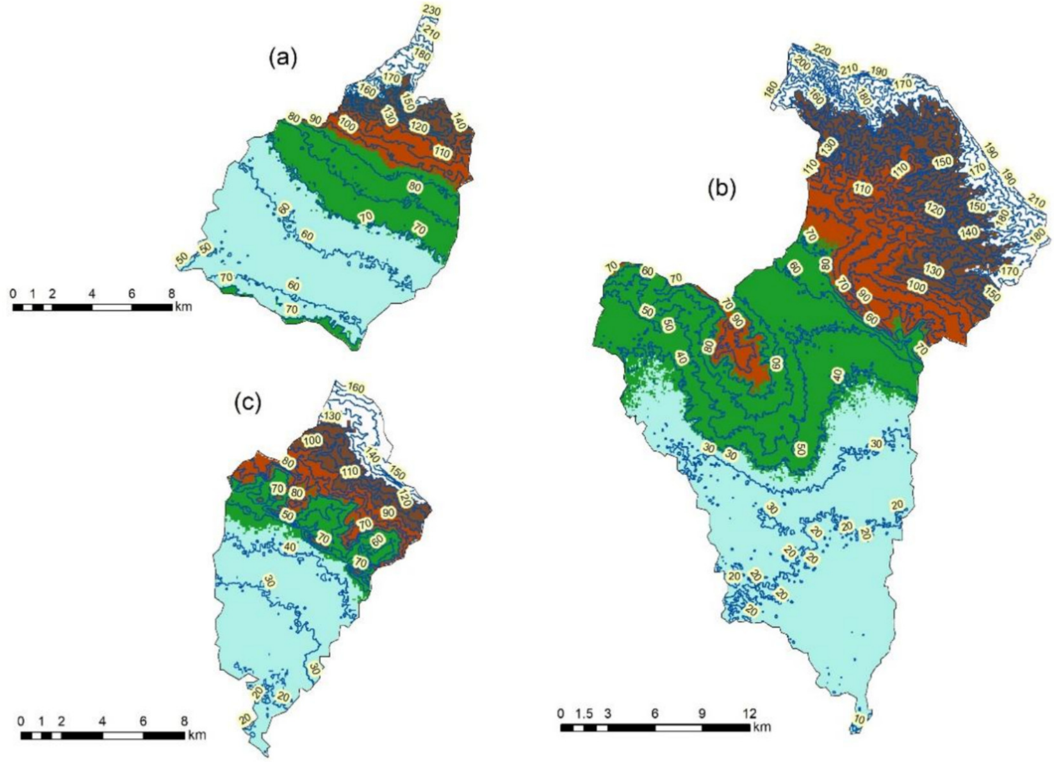

Fig. 3. Contour lines for the Al-Zubaidat area watersheds.

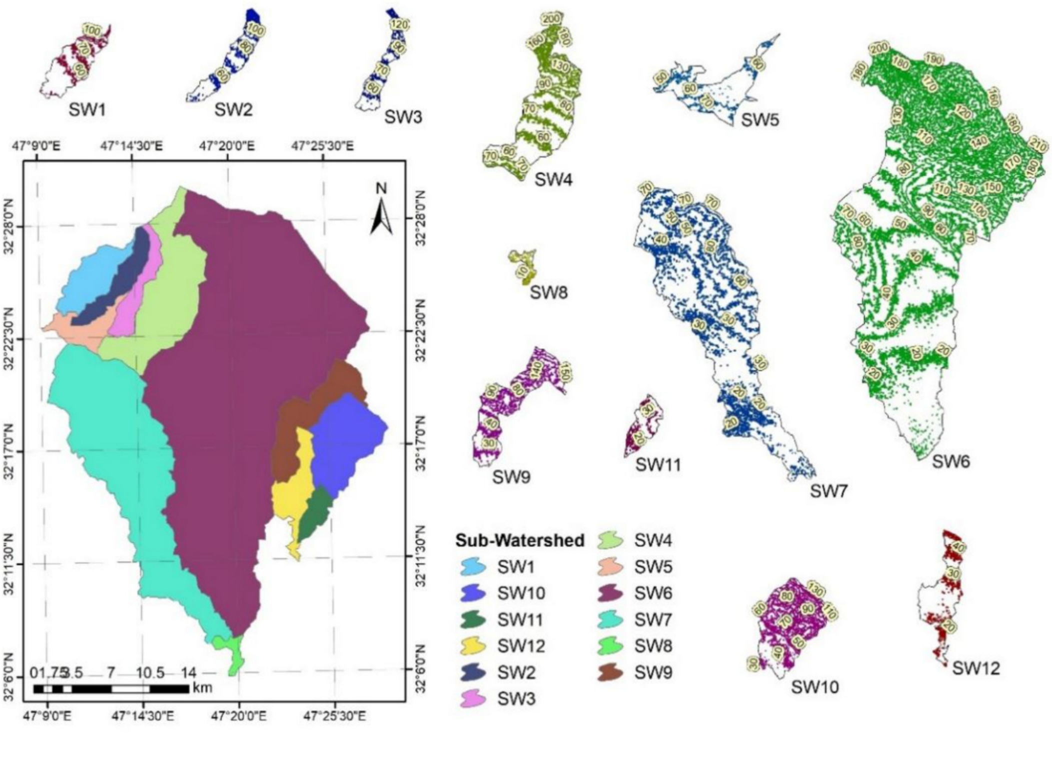

Fig. 4. Contour lines for the Al-Zubaidat area sub-watersheds.

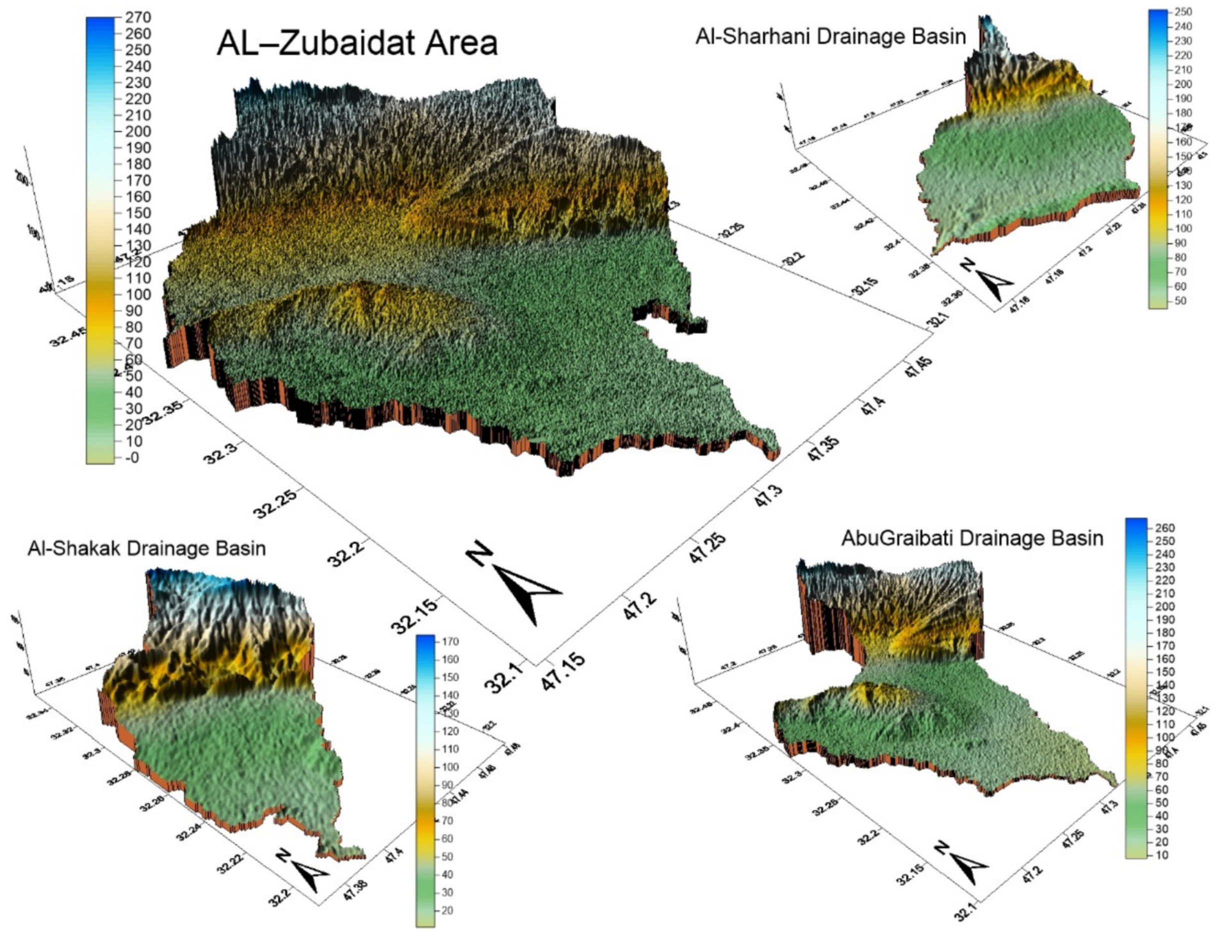

Fig. 5. 3D Terrain view of the Al-Zubaidat area.

Al-Shakak (Figs. 1 and 2). The maximum elevation in the study area is 240 m.a.s.l., while the minimum is 20 m.a.s.l., with a gradient descending from north to south (Figs. 3–6).

The study area comprises geological formations from various periods. The Bai Hassan Formation comprises rock deposits and conglomerates resulting from erosion. This formation is prominently displayed with significant thickness in the northern section of the study area (Fig. 7a). The stratigraphic column of this formation reveals that the lower section comprises layers of limestone, while the upper section consists of predominantly flat clay layers, attaining a thickness of 580 m (Al-Jiburi, 2005). Sheet run-off deposits are distributed throughout the central regions of the study area. The upper strata of these deposits originate from the Holocene epoch, indicating that their formation commenced in the early Pleistocene epoch. The formation of these deposits is associated with the deposition of alluvial fans located in the northern and northeastern sectors of the eastern Al-Jazira region, situated north of the study area (Al-Salih & Al-Kubaisi, 2016).

Aeolian deposits are distributed in areas adjacent to the Bai Hassan Formation, extending in a longitudinal strip of up to 31.431 km and covering an area of 124.559 km^2 (Table 1). These deposits comprise fine sand and silt, attaining an average elevation of 5 m. These deposits were created by wind activity that transported fine sediments from the adjacent floodplain areas (Fig. 7a). Depression-fill deposits accumulate in widely spaced, shallow depressions, which are frequently filled with rainwater. The Al-Sanaf Marsh is the primary depression that is contiguous with and intersects this formation. The deposits comprise silty clay and silty sand, with an average thickness of 1 m and an area of 85.514 km^2.

The study area is classified as arid and semi-arid according to the Koppen climate classification (Al-Hasani et al., 2024a, 2024b). It is characterized by two primary seasons: the hot season, which lasts from April to October, and the cold season, roughly from November to March (Al-Hasani et al., 2025). The summer season is defined by elevated temperatures and aridity, particularly during June, July, and August, with average temperatures of 41.5 °C, 48.3 °C, and 47.7 °C, respectively (Fig. 8). Winter is characterized by moderate temperatures that tend to decline (Al-Hasani et al., 2024a, 2024b). Winter month temperature averages decline, with December, January, and February recording 13.9 °C, 12.2 °C, and 14.8 °C, respectively.

The precipitation in the study area is characterized by its seasonal occurrence, with extended periods of rainfall (Maaroof & Kareem, 2020). Rainfall in the study area occurs from October to May, with an annual average of 12 mm. Precipitation during

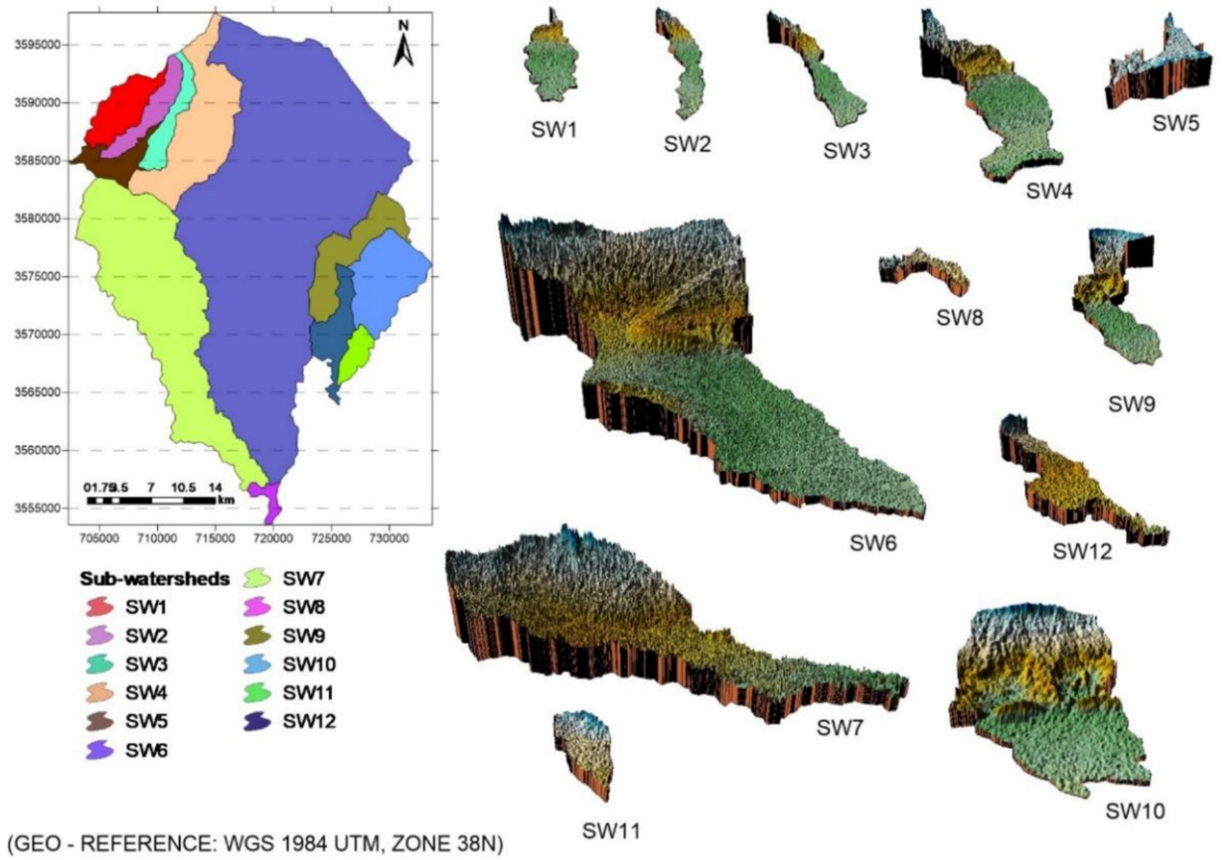

Fig. 6. Sub-watersheds 3D models of the Al-Zubaidat area.

this period is inconsistent (Maaroof et al., 2023), with the highest total of 31.1 mm in January and the lowest total of 8.8 mm in October. Subsequently, monthly rates commence a decline, beginning in February at 32.4 mm. Monthly precipitation rates commence a decrease in April, attaining 18.3 mm, after which rainfall ceases. The precipitation in the study area exhibits annual and monthly variability (Agha & Şarlak, 2016). The yearly mean wind speed in the study area is 3.6 m/s, with summer wind speeds (June, July, and August) reaching 5.4 m/s, 5.4 m/s, and 4.7 m/s, respectively. The mean wind velocity diminishes during winter (November, December, and January), attaining values of 2.8, 2.7, and 2.5 m/s, respectively.

2.2. Data processing

This research employed a geospatial analysis methodology grounded in geoinformatics. A series of procedures was implemented to construct the research. A comprehensive geodatabase concerning the study area was assembled and integrated into the geographic information system, encompassing geological, geomorphological, and hydrological data (Maaroof, 2024). Classification of the spatial features in procedure 1, was conducted by utilizing a diverse array of topographic, geological, geomorphological, and hydrological maps published by the Iraqi General Authority for Survey and the Iraqi Geological Survey at multiple scales (1:1,000,000, 1:250,000, 1:100,000, 1:25,000). Geospatial alignment of data from procedures 1 and 2 utilized the Landsat ETM+ satellite imagery for the United States in 2021, alongside the digital elevation model data of the SRTM type (Maaroof, Al-Abdan, & Kareem, 2021). Geodiversity was categorized based on the physical factors and processes that generated it, according to international standards. A conclusive classification of geodiversity features in maps, field photographs, and geodatabases was developed and illustrated by tables to elucidate the geodiversity within the study area (Fig. 9). The layers were digitally processed using ArcGIS V.10.8, ArcGIS Pro V.3.1, ArcGIS Earth V.2.1, QGIS V.3.12.1, Global Mapper V.11, Surfer V.21, and SAS Planet V.19.1 software.

The study area comprises numerous landforms arranged according to geomorphological factors and processes. Their identification and dimensional measurements were conducted through the analysis of satellite imagery and digital elevation models, along with an examination of topographic and geomorphological maps provided by the Iraqi Geological Survey. The geomorphometric diversity of the Al-Zubaidat area watersheds was analyzed utilizing a series of parameters. The parameters offered precise insights into the geomorphometric attributes of the study area's primary and secondary river drainage basins

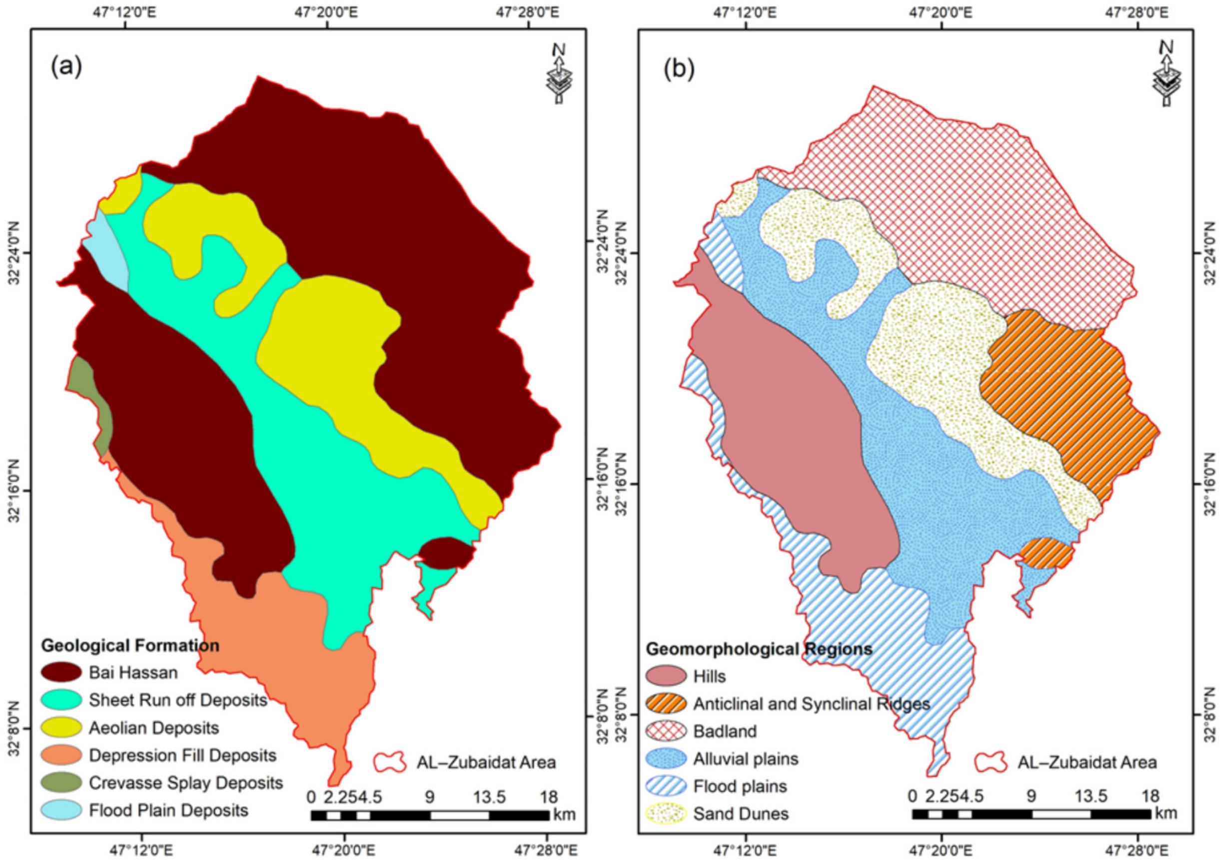

Fig. 7. a. Geological formation. b. Geomorphological regions of Al-Zubaidat area.

(Table 2). The slope diversity of the Al-Zubaidat area watersheds was examined using topographic data from the digital elevation model, terrain classification into elevation categories, determination of slope orientations, and analysis of terrain cross-sections.

3. Results

3.1. Landforms diversity

3.1.1. Hills

The hills in the study area are dome-shaped with steep slopes, covering an area of 130.779 km^2 and constituting 16.716% of the study area (Table 3; Figs. 7b, 10a). These hills have withstood erosion and weathering processes, forming after the removal of softer rock formations. The hills comprise the majority of the badlands in the study area, manifesting as small chains that extend along the floodplain region (Maaroof & Kareem, 2023). The study area features two hills: the first type is widely spaced, isolated, and low in elevation, while the second type is closely situated, intersected, and distinguished by its height and steep gradient. The geological formations of these hills originate from the Tertiary period (Bai Hassan Formation) and comprise limestone, gypsum, and gravel of varying sizes.

Table 1
Era, area, and percentage of geological formations at the Al-Zubaidat area.

Geological formation	Era	Area (km^2)	Percentage
Bai Hassan	Pliocene	393.478	50.295%
Sheet run-off deposits	Holocene	164.756	21.059%
Aeolian deposits	Pleistocene	124.559	15.921%
Depression fill deposits	Pleistocene	85.514	10.930%
Crevasse sply deposits	Pleistocene	6.383	0.817%
Flood plain deposits	Pleistocene	7.618	0.975%

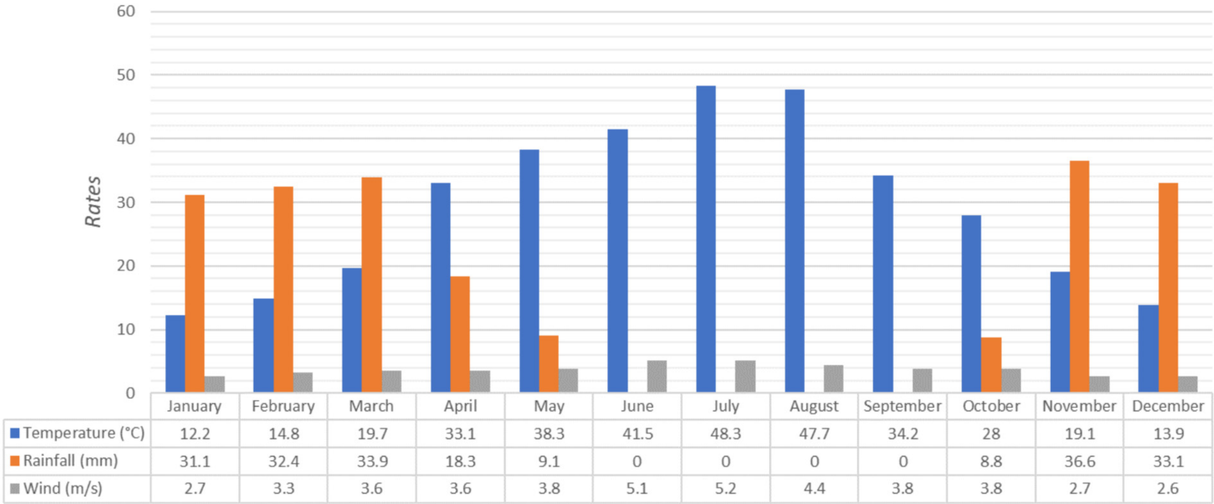

Fig. 8. Temperature, rain, and wind rates in the study area, according to Amarah Climatic Station data (1990–2020).
Source: Iraq | World Meteorological Organization (wmo.int).

3.1.2. Fault scarps

Cracks in the earth's crust have formed on the rock surfaces within the study area, covering an expanse of 84.410 km^2, which constitutes 10.789% (Table 3) and (Figs. 7b, 10b). Fault scarps are present in all rock types, but are most prominent in the stratified sedimentary rocks that define the study area (Sissakian & Fouad, 2015). Fault scarps are abundantly distributed in the eastern sections of the Al-Zubaidat area, resulting from faulting processes throughout the region's geological history (Fouad, 2010). These scarps are distinguished by their linearity and longitudinal extension, oriented in a southeast-northwest direction, and formed after faulting processes that were influenced by erosion and sedimentation.

3.1.3. Valleys

Valleys represent one of the most prevalent geomorphological features in the study area. Fluvial processes sculpted many valleys due to river drainage conditions during the Quaternary period (Maaroof, 2022a, b). Certain valleys have desiccated due to climate change and fall within the semi-desert classification (Figs. 2, 10c, 11).

3.1.4. Badland

This landform is a result of significant erosion caused by precipitation and flowing water in arid and semi-arid regions. In regions with plentiful rainfall, torrents erode fragile rocks, transforming the landscape into gorges and crevices punctuated by

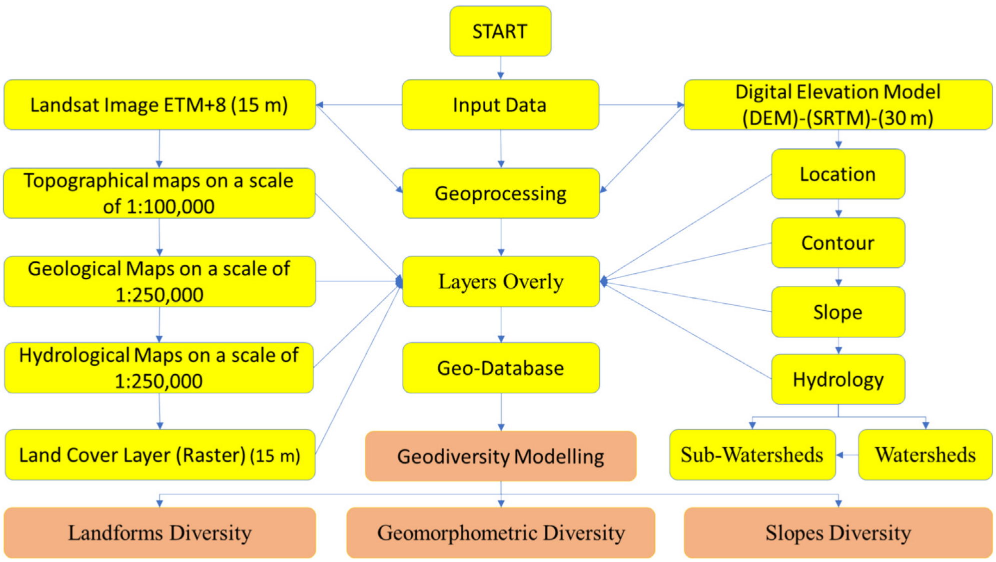

Fig. 9. Information flowchart of methodology.

Table 2
Parameters used to measure the geomorphometric diversity of the watersheds and sub-watersheds in the Al-Zubaidat area.

Parameters	Units	Formula	Description	Reference
Circulatory ratio (R_c)	%	$R_c = 4\pi A/P^2$	A: basin area (km^2); P: perimeter (km)	(Strahler, 1957)
Elongation ratio (R_e)	%	$R_e = \sqrt[2]{(A/\pi)}/L_b$	A: basin area (km^2); L_b: basin length (km)	(Schumm, 1963)
Form factor (F_f)	%	$F_f = A/(L_b)^2$	A: basin area (km^2); L_b: basin length (km)	(Horton, 1945)
Relief ratio (R_h)	m/km	$R_h = H/L_b$	H: the difference between the highest and lowest levels; L_b: basin length (km)	(Schumm, 1956)
Ruggedness number (R_n)	km	$Rn = H^*D/1,000$	H: the difference between the highest and lowest levels; D: drainage density	(Strahler, 1957)
Texture ratio (T)	streams/km	$T = \mathrm{Nu}/P$	Nu: the number of tributaries in the drainage basin; P: The length of the perimeter of the drainage basin	(Strahler, 1954)
Stream orders (U)	Orders	Hierarchical rank	–	(Horton, 1945)
Stream length (Lu)	km	Length of stream	Main channel length of the stream (km)	(Horton, 1945)

jagged outcrops and cliffs (Maaroof et al., 2025). The badlands are located in the northern region of the study area within the Bai Hassan Formation, characterized by a sequence of sandstone, clay, and siltstone strata interspersed with conglomerates, covering an area of 178.277 km^2 and constituting 22.788% of the total study area (Table 3, Figs. 7b, 10d).

3.1.5. Alluvial plain

This plain comprises flat terrain covered by sediments of diverse coarseness, spanning an area of 164.755 km^2, constituting 21.060% (Table 3) and (Figs. 7b, 10e). It is comparatively low, somewhat near the baseline level. Its gentle incline distinguishes this plain and encompasses various geomorphological features, including meanders, alluvial fans, wetlands, and lakes.

3.1.6. Alluvial fans

This landform is created at the transition zones between the steep slopes to the north and northeast of the study area (Fig. 10f) and the neighboring low-lying regions, characterized by their gentle gradients, such as plains and valley bottoms. Alluvial fans form when rivers cascade over steep terrains, transporting substantial quantities of sediment (Al-Jiburi & Al-Basrawi, 2011). As the flow velocity of these rivers abruptly diminishes upon reaching the adjacent low-lying regions, they deposit most of their sediments, forming alluvial fans that extend throughout the northern study area (Sissakian, Jab'bar, & Jabbar, 2014).

3.1.7. Flood plain

The floodplain is situated in the western and southwestern regions of the study area, encompassing an area of 99.531 km^2, which accounts for 12.722% of the total study area (Table 3; Fig. 7b). It is among the most level surface characteristics in the study area. This plain was created by the deposition of sediments carried by valleys from the elevated northern regions. This plain inclines in a northeast-southwest orientation, aligning with the overall gradient of the study area (Yacoub, 2011b).

3.1.8. Meander

The meander in the research area is a consequence of lateral erosion induced by the river, influenced by prevailing geomorphological processes (Maaroof & Kareem, 2022). The presence of a bank characterized by a high ratio of sand and silt and a low ratio of clay is the principal factor contributing to the formation of the meander in the examined region (Fig. 10g). This bank vigorously reacts to lateral erosion processes, forming an external arch or concavity characterized by a steep, deep, narrow bank.

3.1.9. Dunes

They encompass extensive regions of the study area, covering 124.556 km^2, which constitutes 15.921% of the total area (Table 3). The geomorphological map reveals two dune areas, with the first located southwest of the Badlands region (Figs. 7b,

Table 3
Area and percentage of geomorphological regions in the Al-Zubaidat area.

Geomorphological regions	Area (km^2)	Percentage
Hills	130.779	16.716%
Fault scarps	84.410	10.789%
Badland	178.277	22.788%
Alluvial plain	164.755	21.060%
Flood plain	99.531	12.722%
Dunes	124.556	15.921%

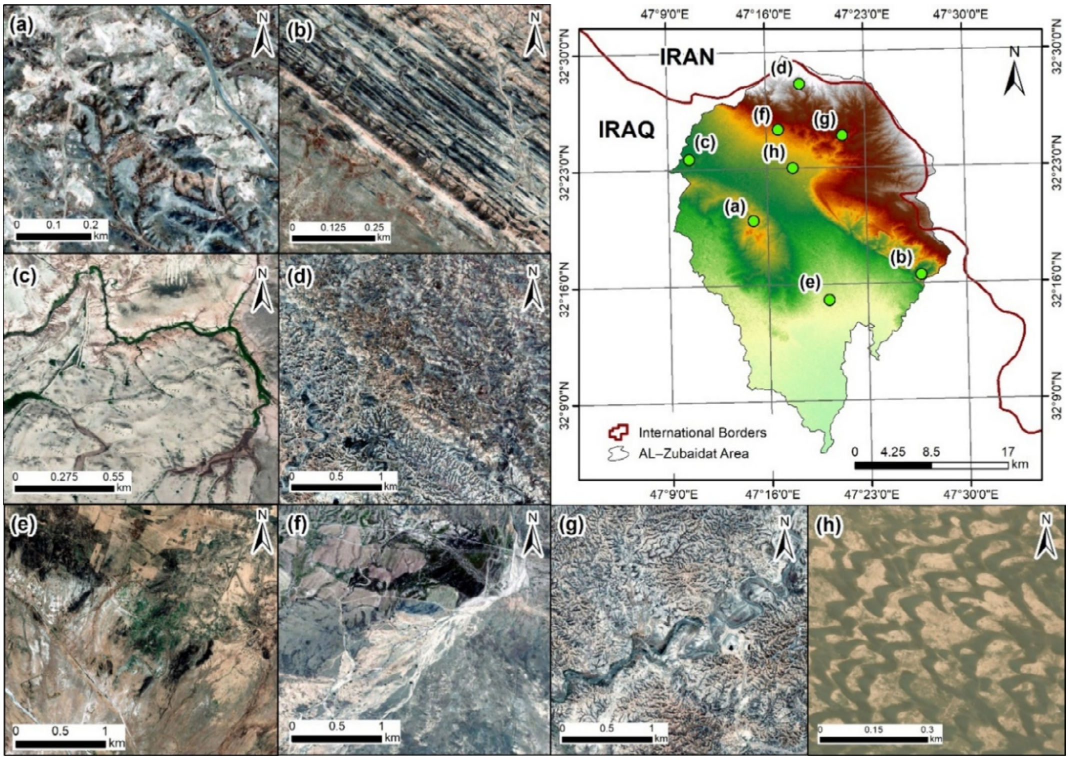

Fig. 10. Landform diversity in the study area. a. Hills. b. Fault Scarps. c. Valleys. d. Badland. e. Alluvial plain. f. Alluvial fans. g. Meander. h. Dunes.

10h). The second dune area is a longitudinal strip west of the fault scarps region (Yacoub, 2010). The study area comprises three types of dunes: longitudinal, barchan, and transverse. The formation of these dunes is likely attributed to variations in surface roughness, resulting in the concentration of sand, particularly in the lower regions (Al-Janabi, Jawad Ali, Al-Taie, & Jack, 1988).

3.2. Geomorphometric diversity

3.2.1. Watershed area (A)

The Al-Zubaidat region encompasses a total area of 782.308 km^2, comprising three principal watersheds (Al-Sharhani, Abu-Ghraibat, and Al-Shakak) and twelve sub-watersheds (see Table 4, Figs. 2, 11). The Abu-Ghraibat watershed is the principal one, encompassing an area of 553.423 km^2, constituting 70.741% of the Al-Zubaidat region. The Al-Sharhani watershed includes a total area of 129.411 km^2, representing a rate of 16.541%, and is the second-largest watershed in the Al-Zubaidat region. The Al-Shakak watershed is the more minor primary watershed in the study area, encompassing an area of 99.485 km^2, which constitutes 12.716% of the region's total area. The sub-watersheds exhibited varying sizes, with sub-watershed 6 (SW6) encompassing an area of 399.893 km^2 and a rate of 51.112, making it the largest sub-watershed in the study area. Sub-watershed 8 (SW8) comprises an area of 4.433 km^2, constituting 0.566% of the total area, and is the smallest sub-watershed within the study area (Table 5, 6, 7, and 8).

3.2.2. Watershed length (L_b)

It is a fundamental geomorphometric variable, as it has numerous correlations in assessing the characteristics of the watershed. Schumm (1956) ascertained this parameter by measuring a line from the downstream point to the apex of the drainage basin. The data in Table 4 indicate that the drainage basins with the most significant area correspond to those with the longest lengths. The Abu-Ghraibat watershed measures 42.355 km, making it the longest in the study area and the largest in the region. The Al-Shakak watershed ranks second, measuring 18.660 km in length. The Al-Sharhani watershed ranks third, measuring 17.094 km in length, despite having a larger area than the Al-Shakak watershed. The Al-Sharhani watershed is distinguished by its circular shape, which contrasts with the longitudinal form of the Al-Shakak watershed. This suggests that the rocks in the source area are of a complex type resistant to water erosion, resulting in no correlation between length and area. The sub-watershed lengths vary, with SW6 being the longest at 41.029 km and SW8 the shortest at 4.203 km (Tables 5, 6; Figs. 2, 11).

3.2.3. Watershed width (W)

The width of the primary watersheds in the study area exhibits variation. The width of the Abu-Ghraibat watershed attains 13.066 km, denoting the maximum value. The minimum width of the Al-Shakak watershed is 5.331 km. The Al-Sharhani

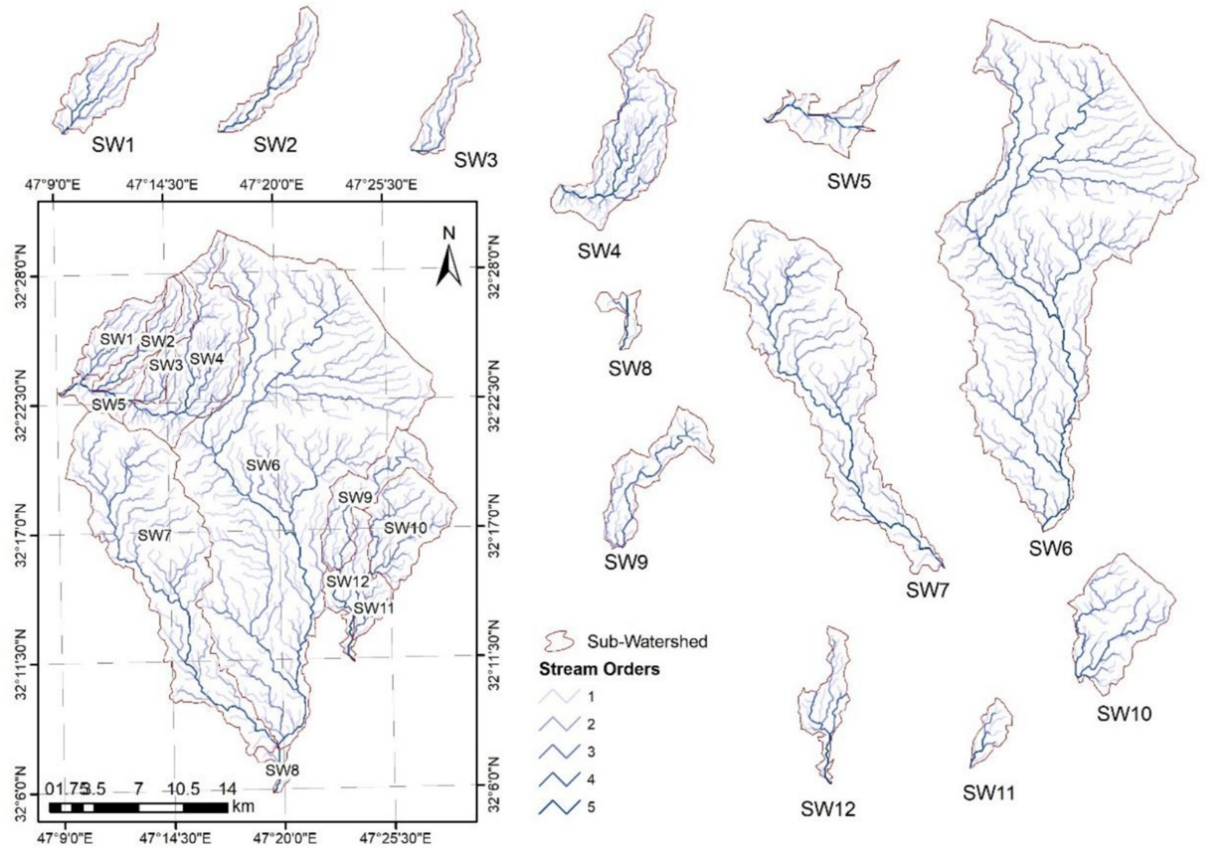

Fig. 11. Sub-watershed drainage networks for the Al-Zubaidat area.

watershed's width averages 7.570 km. The width values of sub-watersheds in the study area exhibit variation, with sub-watershed 6 (SW6) recording a maximum width of 9.746 km. In contrast, sub-watershed 8 (SW8) records a length of 1.054 km, the shortest among the sub-watersheds, while the others exhibit significant variability in their measurements due to variations in rock quality and differing impacts of river erosion processes.

3.2.4. Watershed perimeter (P)

This parameter is related to various geomorphometric characteristics for assessing watershed dimensions. It relates to the coefficients of the Circulatory Ratio (R_c), Form Factor (F_f), and Elongation Ratio (R_e) of the watersheds. The increase in the perimeter correlates directly with the expansion of the area (Abboud & Nofal, 2017). The perimeter measurements for the primary watersheds (Al-Sharhani, Abu-Ghraibat, and Al-Shakak) were 56.793, 142.454, and 53.949 km, respectively. The sub-watersheds exhibited varying values, with sub-watershed 6 (SW6) attaining the highest measurement of 117.093 km, while sub-watershed 8

Table 4
Geomorphometric diversity of the main watersheds of the Al-Zubaidat area.

Parameters	Values		
	Al-Sharhani watershed	Abu-Ghraibat watershed	Al-Shakak watershed
Basin area (A) (km^2)	129.411	553.423	99.485
Basin length (L_b) (km^2)	17.094	42.355	18.660
Basin width (W) (km)	7.570	13.066	5.331
Basin perimeter (P) (km)	56.793	142.454	53.949
Circulatory ratio (R_c)	2.278	3.884	1.844
Elongation ratio (R_e)	0.751	0.626	0.603
Form factor (F_f)	0.442	0.308	0.285
Relief ratio (R_h)	11.700	5.666	9.110
Ruggedness number (R_n)	0.007	2.387	5.572
Texture ratio (T)	7.078	5.306	4.226

Table 5
Areas and their percentages of watersheds and sub-watersheds in the Al-Zubaidat area.

Values of watersheds		
Al-Sharhani watershed	Abu-Ghraibat watershed	Al-Shakak watershed
16.541%	70.741%	12.716%

Values of sub-watersheds											
SW1	SW2	SW3	SW4	SW5	SW6	SW7	SW8	SW9	SW10	SW11	SW12
2.770%	2.063%	1.837%	8.118%	1.753%	51.112%	19.060%	0.566%	4.056%	5.053%	1.081%	2.525%

(SW8) recorded the lowest at 13.834 km. Elevated values of this parameter in specific watersheds signify heightened activity and progression of geomorphological processes.

3.2.5. Watershed circularity ratio (R_c)

The circularity ratio measures the proximity of the watershed's shape to a perfect circle. High circularity ratio values are indicative of round watersheds, whereas low values suggest more elongated shapes (Prasannakumar, Shiny, Geetha, & Vijith, 2011). The circularity ratio for the Abu-Ghraibat watershed attains 3.884%, the highest among the principal watersheds. The parameter's value for the Al-Shakak watershed is 1.844%, representing the lowest recorded value to date. The circularity ratio ranges from 0.464 % in SW5 (the lowest) to 3.415% in SW6 (the highest).

3.2.6. Watershed elongation ratio (R_e)

This parameter was introduced by Schumm in 1963. The watershed approaches a rectangular configuration. The values of this parameter range from 0 to 1. The proximity of the values to zero correlates with the elongation of the watershed. Values exceeding 1 indicate that the watershed is nearing a circular configuration (Arefin, Mohir, & Alam, 2020). The elongation ratio for the Al-Sharhani watershed attains 0.751%, the highest recorded value, indicating proximity to a circular form. In contrast, the Al-Shakak watershed records a value of 0.603%, the lowest among the watersheds, signifying a high elongation ratio. The coefficient value for SW10 is 0.726%, the highest among sub-watersheds, whereas for SW2, it was 0.387%, the lowest.

3.2.7. Watershed form factor (F_f)

This parameter identifies whether the watershed's shape diverges from or converges towards a triangular form. Minimal values of this parameter suggest that the watershed is nearing a triangular configuration and vice versa. The form factor for the Al-Shakak watershed is 0.285%, the lowest among all watersheds, indicating a shape that approximates a triangle. The Al-Sharhani watershed attains a value of 0.442%, the highest figure signifying its deviation from the triangular form. The sub-watershed SW3 exhibits the lowest values at 0.115%, suggesting a near-triangular configuration.

3.2.8. Watershed relief ratio (R_h)

This parameter identifies the topographic system of the area. The volume of transported sediments escalates with heightened relief, forming various erosional and depositional landforms (Resmi, Babeesh, & Achyuthan, 2019). The relief ratio enables the assessment of the watershed's hydrological conditions. The flood intensifies as the relief ratio rises, attributable to the water current's arrival velocity. This exacerbates the effects of water erosion and the concomitant transport of substantial sediment quantities (Fenta, Yasuda, Shimizu, Haregeweyn, & Woldearegay, 2017). The relief ratio for the Al-Sharhani watershed attains 11.700 m/km, the highest among all. The Abu-Ghraibat watershed recorded a value of 5.666 m/km, the lowest observed. The sub-watersheds exhibited diverse values for this parameter, with SW2 recording the highest at 14.539 m/km and SW5 the weakest at 1.973 m/km.

Table 6
Geomorphometric diversity of the sub-watersheds of the Al-Zubaidat area.

Parameters	Values										
	SW1	SW2	SW3	SW4	SW5	SW6	SW7	SW8	SW9	SW10	SW11	SW12
Area (A) (km^2)	21.679	16.146	14.373	63.518	13.720	399.893	149.128	4.433	31.740	39.534	8.460	19.759
Basin length (L_b) (km^2)	10.188	11.692	11.175	19.416	10.136	41.029	30.707	4.203	13.577	9.767	5.923	12.581
Width (W) (km)	2.127	1.380	1.286	3.271	1.353	9.746	4.856	1.054	2.337	4.047	1.428	1.570
Perimeter (P) (km)	26.287	26.963	26.922	50	29.533	117.093	83.831	13.834	38.112	28.705	14.721	34.933
Circulatory ratio (R_c)	0.824	0.598	0.533	1.270	0.464	3.415	1.778	0.320	0.832	1.377	0.574	0.565
Elongation ratio (R_e)	0.515	0.387	0.382	0.463	0.412	0.550	0.448	0.565	0.468	0.726	0.554	0.398
Form factor (F_f)	0.208	0.118	0.115	0.168	0.133	0.237	0.158	0.250	0.172	0.414	0.241	0.124
Relief ratio (R_h)	9.815	14.539	15.212	9.785	1.973	6.093	2.279	2.379	10.311	14.333	3.376	5.563
Ruggedness number (R_n)	8.718	14.073	15.833	8.586	1.476	3.005	1.195	1.284	6.431	8.178	2.433	3.913
Texture ratio (T)	2.586	1.854	1.671	3.84	1.286	4.569	2.528	0.650	1.600	3.553	1.154	1.431

Table 7
Stream orders for Al-Zubaidat area watersheds.

Watersheds	Stream orders							Percentage
	1st	2nd	3rd	4th	5th	6th	Total streams	
Al-Sharhani watershed	204	108	44	31	15	–	402	29.004%
Abu-Ghraibat watershed	380	177	86	62	47	4	756	54.545%
Al-Shakak watershed	115	54	40	15	4	–	228	16.450%
Total streams	699	339	170	108	66	4	1,386	100%
Percentage	50.432%	24.458%	12.265%	7.792%	4.761%	0.288%	–	100%

3.2.9. Watershed ruggedness number (R_n)

This parameter quantifies the correlation between topography and the density of watershed discharge. The ruggedness value escalates with the augmentation of relief and the extension of the stream's length. Strahler (1957) observed that ruggedness values ranged from 0.06 in low-relief watersheds to over 1 in high-relief watersheds (Strahler, 1957). The ruggedness value for the Al-Shakak watershed is 5.572 km^2, indicating a relatively high measurement within the study area. This elevated value indicates a favorable trend in stream lengths, despite the watershed's relatively small area compared to its peers. The elevated value is attributable to the limestone formations within the watershed, which exhibit diverse reactions to water erosion processes. The sub-watershed measurements range from the value above, with SW2 attaining 14.073 km, a notably high figure, while SW8 records the lowest value at 1.284 km.

3.2.10. Texture ratio (T)

This parameter measures the distance between the streams or their closeness to each other. It indicates the quality of the topography, the degree of erosional development of the watershed, and its efficiency. Smith (1950) classified watersheds by topographic texture value into four classes: 0–4 (coarse), 4–10 (medium), 10–15 (fine), and more than 15 (very fine) (Strahler, 1954). The value of the topographic texture is 4.226 streams/km for the Al-Shakak watershed, which is a medium value according to Smith's (1950) scale. It reaches 7.078 streams/km for the Al-Sharhani watershed, which is also a medium value.

3.2.11. Watershed stream orders (U)

The stream orders have been classified according to the method developed by Strahler (1954). According to this method, the first streams of waterways that do not receive tributaries from above are classified as first-order tributaries; when two streams of the first order meet, a stream of the second order is formed (Umrikar, 2017). When two streams of the second order meet, a stream of the third order is formed, and so on for the rest of the other orders (Dinagara Pandi et al., 2017). The total number of stream orders for the study area watersheds was six, and their numbers varied from one order to another. According to Horton's (1945) law for waterways, they follow orders in a geometric sequence, whose maximum limit is the first order, and then decrease as the order increases. The numbers of the first, second, and third orders were 699, 339, and 170, respectively, accounting for 50.432%, 24.458%, and 12.265%, respectively. The rest of the orders came in smaller numbers and percentages (Tables 7 and 8).

3.2.12. Watershed stream length (L_u)

The total stream length for the study area is 1,252.312 km, with large watersheds comprising most of the length. The stream lengths of the Abu-Ghraibat watershed reach 784.14 km, accounting for 62.615% of the total. The Al-Sharhani watershed came in second place, with a total stream length of 292.231 km, representing 23.335% of the total stream length. The Al-Shakak watershed

Table 8
Stream orders for Al-Zubaidat area sub-watersheds.

Watersheds	Stream orders						Percentage
	1st	2nd	3rd	4th	5th	Total streams	
SW1	35	17	12	5	–	69	4.931%
SW2	27	12	5	4	–	51	3.625%
SW3	23	15	5	4	–	47	3.263%
SW4	97	55	21	19	–	192	13.923%
SW5	22	9	1	5	15	39	2.755%
SW6	269	124	68	44	30	535	38.796%
SW7	107	52	18	18	17	212	15.373%
SW8	4	1	4	–	–	9	0.652%
SW9	31	14	15	2	–	62	4.423%
SW10	52	27	21	3	–	103	7.396%
SW11	9	4	4	–	–	17	1.232%
SW12	23	9	14	4	–	50	3.625%
Total streams	699	339	188	108	62	1,386	100%

Table 9
Stream lengths are according to the stream orders for the Al-Zubaidat area watersheds.

Watersheds	Stream lengths (km)							Percentage
	1st	2nd	3rd	4th	5th	6th	Total streams	
Al-Sharhani watershed	153.494	82.137	33.004	17.115	6.481	–	292.231	23.335%
Abu-Ghraibat watershed	384.144	204.495	80.614	63.053	48.165	3.669	784.14	62.615%
Al-Shakak watershed	81.815	46.707	33.619	9.422	4.378	–	175.941	14.049%
Total streams	619.453	333.339	147.237	89.59	59.024	3.669	1252.312	100%
Percentage	49.464%	26.617%	11.757%	7.153%	4.713%	0.292%	–	100%

comes in last place, with a total stream length of 175.941 km, representing a percentage of 14.049%. Sub-watersheds also vary in length, with SW6 taking first place, boasting a total stream length of 562.833 km, which accounts for 44.956% of the total stream length. SW7 is in second place, with a total stream length of 213.428 km, with a percentage of 17.047. The rest of the sub-watersheds deviate from the above values, with the lowest being SW8, which has a total stream length of 7.876 km, accounting for 0.629% (Tables 9 and 10).

3.3. Slope diversity

3.3.1. Slope categories

The watersheds in the study area are classified into five slope categories (see Tables 11 and 12 and Figs. 12 and 13). Each category is defined by slope characteristics corresponding to the geomorphological stage of the watershed throughout its entirety. The slope classifications in watersheds and sub-watersheds differed based on the effects of geomorphological processes, phases, climate, and geological structure (Maaroof, 2022a). The slope category ranging from 0 to 0.686 covers an area of 252.82 km^2, accounting for 46.638% of the Abu-Ghraibat watershed. This proportion represents the highest value among the considered slope-category areas in this context. In contrast, the slope category from 5.187 to 10.415 covers an area of 1.693 km^2, making up 1.354% of the Al-Sharhani watershed, which is the lowest value. Notably, there are variations in slope categories across sub-watersheds. In sub-watershed SW6, the slope category from 0 to 1.512 occupies an area of 150.812 km^2, representing 37.982% of the sub-watershed area, marking the highest recorded proportion. Meanwhile, in sub-watershed SW8, the slope category from 5.407 to 10.689 covers an area of 0.110 km^2, accounting for 2.692% of the sub-watershed area, which is the minimum value observed.

3.3.2. Slope directions

The study area exhibits a gradual slope from north to south and southwest, representing its overall gradient. The study area encompasses local slopes in the north, east, south, and west, as well as secondary directions. There is variability in the regions and percentage gradients of slopes within watersheds. The western slopes (247.5–292.5) encompassed an area of 61.789 km^2, representing 11.164% of the Abu-Ghraibat watershed, the highest recorded value. Flat (−1) slopes attained an area of 4.324 km^2, constituting 3.341% of the Al-Sharhani watershed, the lowest recorded value (Table 13 and Fig. 14).

3.3.3. Slope parts

The slope segment is the portion of the sloped cross-section where the inclination angle remains uniform. Analyzing the slope component enables the determination of the uniformity of the overall terrain cross-section length and the geomorphometric attributes of the slope elements. Table 14 reveals a discernible variation in the numbers and lengths of the slope segments. In the

Table 10
Stream lengths are according to the stream orders for the Al-Zubaidat area sub-watersheds.

Watersheds	Stream lengths (km)						Percentage
	1st	2nd	3rd	4th	5th	Total streams	
SW1	26.747	13.709	8.188	1.039	–	49.683	3.968%
SW2	16.668	9.548	4.398	5.424	–	36.038	2.878%
SW3	17.037	12.178	3.123	0.714	–	33.052	2.640%
SW4	76.626	41.280	17.173	8.448		143.529	11.464%
SW5	16.403	5.419	0.121	1.488	6.48	29.911	2.389%
SW6	282.338	140.392	62.229	47.461	30.413	562.833	44.956%
SW7	98.881	62.819	18.385	15.592	17.751	213.428	17.047%
SW8	2.924	1.283	3.669	–	–	7.876	0.629%
SW9	27.138	12.867	15.536	0.027	–	55.568	4.438%
SW10	29.565	21.301	14.998	0.428	–	66.292	5.295%
SW11	8.016	4.051	3.085	–	–	15.152	1.210%
SW12	16.889	8.363	8.96	4.378	–	38.59	3.082%
Total streams	619.232	333.210	159.865	84.999	54.644	1251.950	100%

Table 11
Slope categories, their areas, and percentages for the Al-Zubaidat area watersheds.

Watersheds	Slope categories (m/km)	Area (km^2)	Percentage
Al-Sharhani watershed	0–0.776	72.858	58.264%
	0.776–1.797	33.750	26.990%
	1.797–3.226	11.601	9.277%
	3.226–5.187	5.144	4.113%
	5.187–10.415	1.693	1.354%
Abu-Ghraibat watershed	0–0.686	252.820	46.638%
	0.686–1.450	154.803	28.556%
	1.450–2.480	85.252	15.726%
	2.480–3.968	40.932	7.550%
	3.968–9.730	8.280	1.527%
Al-Shakak watershed	0–0.858	47.418	49.847%
	0.858–1.881	23.148	24.334%
	1.881–3.102	15.760	16.567%
	3.102–4.917	6.861	7.212%
	4.917–8.415	1.938	2.037%

Terrain cross-section of the Abu-Ghraibat watershed, there are 216 slope segments, with an average length of 0.087 in the headwater region, representing the highest value documented in the study area. The terrain cross-section of the Al-Sharhani watershed consists of 31 slope segments. In the headwater region, these segments have an average length of 0.085, which represents the minimum value among the relevant measurements. The rise in the number of slope segments in specific terrain cross-sections of the study area's watersheds is attributed to the water erosion processes to which they are subjected, particularly since these regions are in the youthful phase of the geomorphological cycle (Figs. 15, 16, and 17).

4. Discussion

We have recognized dome-shaped hills, valleys, and badlands. The region encompasses 782.308 km^2 and includes three main watersheds (Al-Sharhani, Abu-Ghraibat, and Al-Shakak) along with 12 subordinate watersheds, primarily defined by fluvial geomorphic features. The advancement of geoheritage, geodiversity, and geoconservation, along with the establishment of geoparks,

Table 12
Slope categories, their areas, and percentages for the Al-Zubaidat area sub-watersheds.

Watersheds	Slope categories (m/km)	Area (km^2)	Percentage	Watersheds	Slope categories (m/km)	Area (km^2)	Percentage
SW1	0–1.130	8.214	39.136%	SW7	0–1.196	52.440	35.697%
	1.130–2.063	6.239	29.726%		1.196–2.152	49.422	33.642%
	2.063–3.194	4.340	20.678%		2.152–3.289	30.787	20.957%
	3.194–5.012	1.951	9.295%		3.289–4.963	11.991	8.162%
	5.012–12.530	0.244	1.162%		4.963–15.249	2.2625	1.540%
SW2	0–1.552	6.425	41.761%	SW8	0–1.131	1.878	45.973%
	1.552–3.246	5.821	37.835%		1.131–2.221	1.351	33.072%
	3.246–5.787	2.038	13.246%		2.221–3.563	0.502	12.288%
	5.787–9.457	0.777	5.050%		3.563–5.407	0.244	5.973%
	9.457–17.998	0.324	2.105%		5.407–10.689	0.110	2.692%
SW3	0–1.536	6.715	49.165%	SW9	0–1.533	10.601	34.482%
	1.536–3.145	4.508	33.006%		1.533–2.839	11.071	36.011%
	3.145–5.632	1.621	11.868%		2.839–4.485	6.159	20.033%
	5.632–9.289	0.594	4.349%		4.485–7.211	2.380	7.741%
	9.289–18.652	0.220	1.610%		7.211–14.479	0.532	1.730%
SW4	0–1.479	25.298	40.685%	SW10	0–1.762	12.297	31.718%
	1.479–2.823	20.610	33.146%		1.762–3.349	13.237	34.143%
	2.823–4.706	11.268	18.121%		3.349–5.376	8.707	22.458%
	4.706–7.799	4.156	6.683%		5.376–8.284	3.568	9.203%
	7.799–17.145	0.847	1.362%		8.284–22.475	0.960	2.476%
SW5	0–1.085	3.895	30.060%	SW11	0–1.102	3.277	40.481%
	1.085–2.020	4.356	33.618%		1.102–1.879	2.324	28.709%
	2.020–2.984	2.911	22.466%		1.879–2.631	1.360	16.800%
	2.984–4.251	1.382	10.666%		2.631–3.734	0.900	11.117%
	4.251–7.688	0.413	3.187%		3.734–6.391	0.234	2.890%
SW6	0–1.512	150.812	37.982%	SW12	0–1.280	7.959	42.368%
	1.512–2.798	123.966	31.221%		1.280–2.475	7.011	37.322%
	2.798–4.462	81.526	20.532%		2.475–4.609	2.988	15.906%
	4.462–7.109	33.664	8.478%		4.609–8.279	0.615	3.273%
	7.109–19.286	7.087	1.784%		8.279–21.766	0.212	1.128%

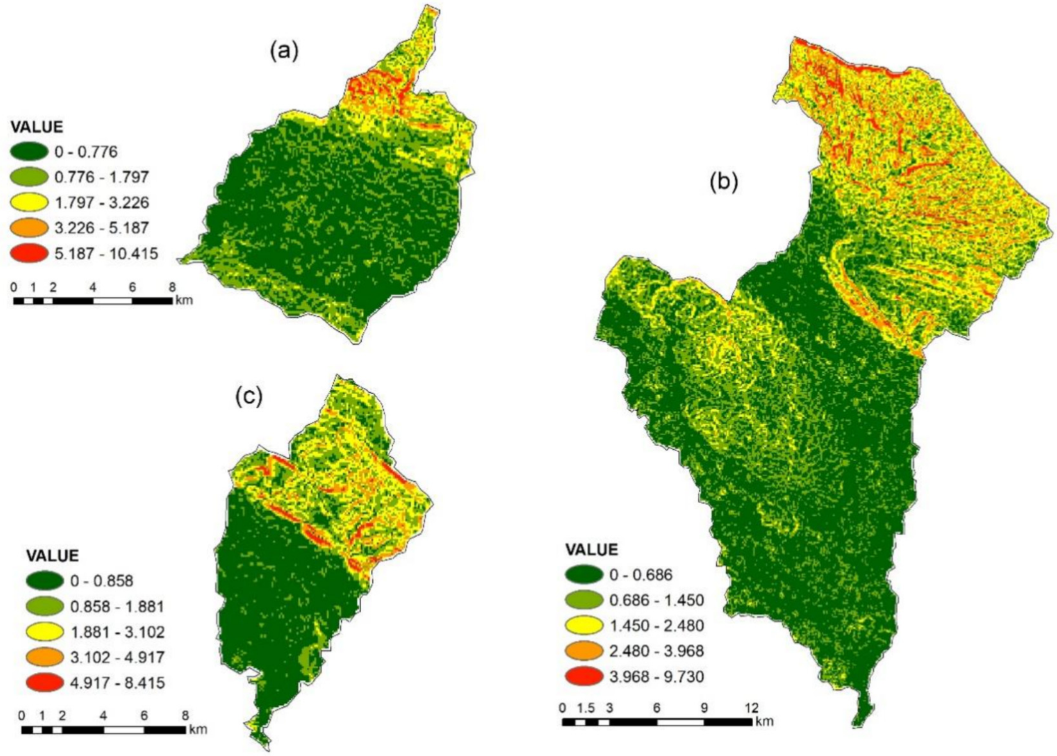

Fig. 12. Slope categories for Al-Zubaidat area watersheds.

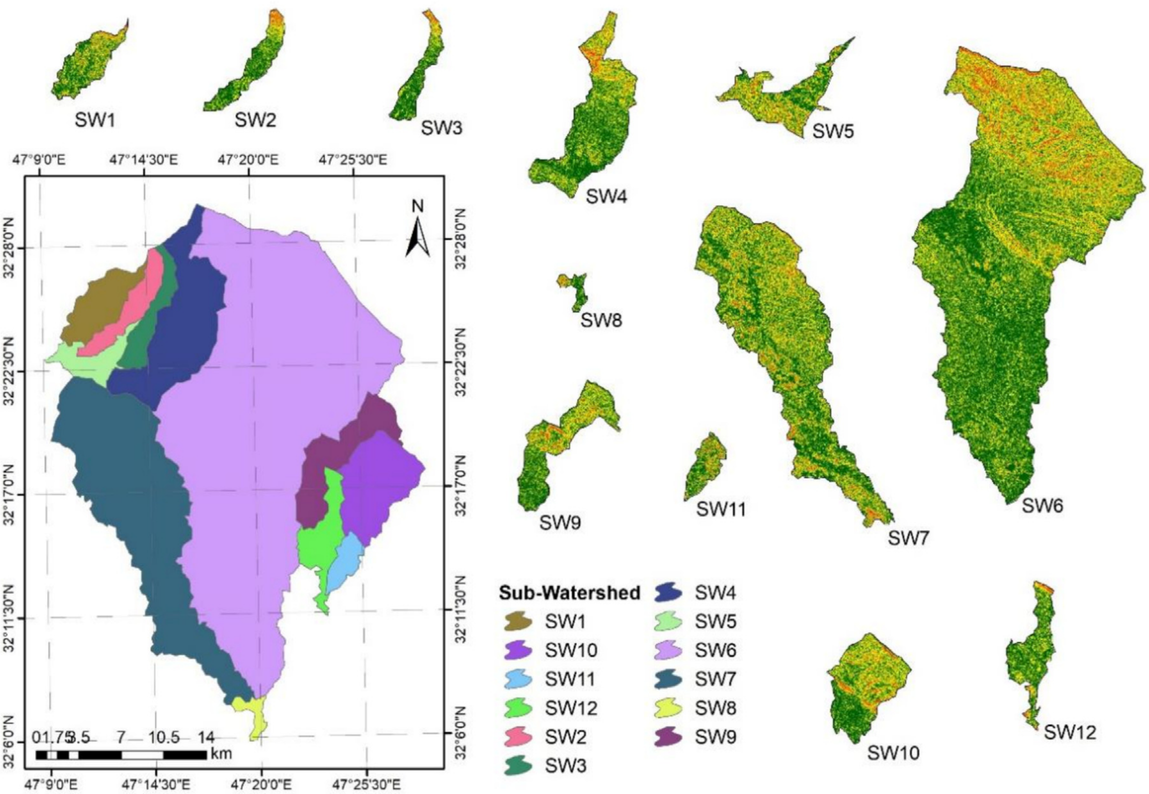

Fig. 13. Slope categories of the Al-Zubaidat area sub-watersheds.

Table 13
Slope directions for Al-Zubaidat area watersheds.

Slope directions	Al-Sharhani watershed		Abu-Ghraibat watershed		Al-Shakak watershed	
	Area (km^2)	Percentage	Area (km^2)	Percentage	Area (km^2)	Percentage
Flat (-1)	4.324	3.341%	11.243	2.031%	4.386	4.409%
North (0−22.5)	13.401	10.355%	57.866	10.456%	7.458	7.496%
Northeast (22.5−67.5)	8.623	6.663%	53.382	9.645%	6.906	6.942%
East (67.5−112.5)	10.279	7.943%	70.366	12.714%	9.354	9.403%
Southeast (112.5−157.5)	11.511	8.895%	77.044	13.921%	13.827	13.899%
South (157.5−202.5)	15.400	11.900%	66.391	11.996%	14.238	14.312%
Southwest (202.5−247.5)	17.523	13.54%	67.147	12.133%	13.202	13.270%
West (247.5−292.5)	21.516	16.626%	61.789	11.164%	11.156	11.214%
Northwest (292.5−337.5)	15.267	11.797%	52.885	9.556%	10.660	10.715%
North (337.5−360)	11.562	8.935%	35.304	6.3793%	8.293	8.336%

offers substantial prospects for promoting sustainable development, advocating sustainable lifestyles, and augmenting the appreciation of natural and cultural diversity while also fostering peace (Quesada-Román, Zangmo, & Pérez-Umaña, 2020). These initiatives are crucial for disseminating geoscience knowledge to policymakers involved in geotourism and conservation across multiple nations, as well as to local stakeholders. In semi-arid and developing regions, particularly in Southeast Asia, there is an urgent need to advance geoheritage research, focusing on geomorphological dynamics and the significant anthropogenic pressures that affect geo- and biodiversity. This emphasis is crucial for enhancing revenue via geotourism, especially for marginalized communities, while protecting their fragile natural resources (Quesada-Valverde & Quesada-Román, 2023).

In their upper layers, the hills in the study area have been exposed to various erosion factors, especially water erosion, due to the weak resistance of some of the rocky parts. This has led to the formation of many waterways that divide them and form these hills, which reached a maximum height of 230 m above sea level. All fault scarps in the study area undergo morphological changes after the faulting processes, as evidenced by many waterways that cut them and sediments on parts of them. The slope of these scarps is steep towards the Al-Shakak drainage basin, with a slope angle ranging between 50° and 60°. The slope of these scarps varies from one place to another, as the slopes are steep in the southeastern range and less steep in the northwestern range (Fouad, 2015). A group of factors, such as the type of rocks and faults, controls the formation of the valleys. Streamways often follow areas of weak rock, where streams merge to form valleys (Sissakian & Fouad, 2015). The rock formations in the badlands vary in hardness; the less resistant rocks are vulnerable to erosion, while the more resistant ones remain as prominent outcrops surrounded by lower areas (Yacoub, 2011a). Several factors contribute to the formation of this plain, the most significant of which is the frequent flooding of rivers (Fouad & Sissakian, 2011).

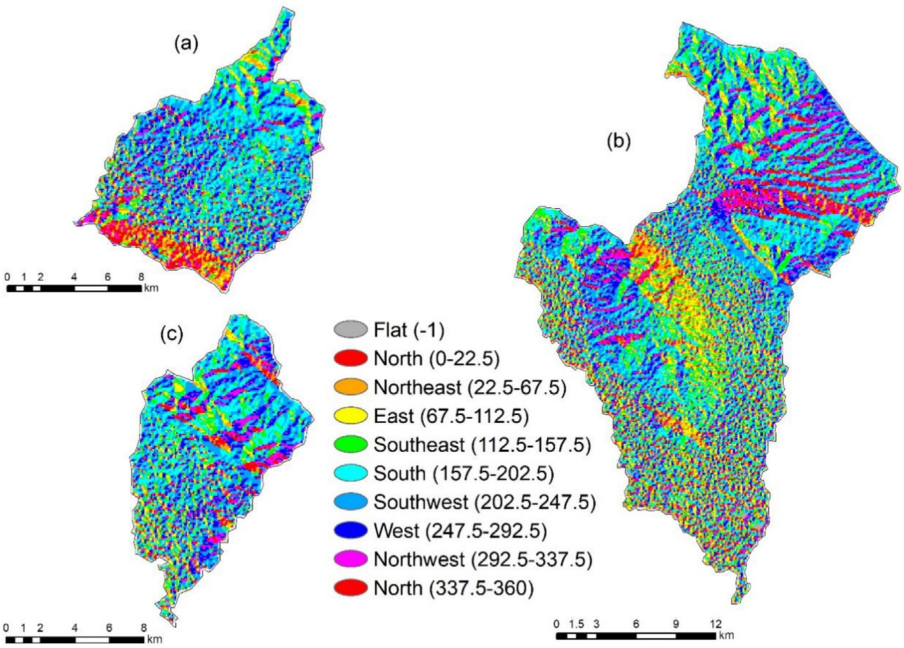

Fig. 14. Slope direction for Al-Zubaidat area watersheds.

Table 14
Slope parts for Al-Zubaidat area watersheds.

Terrain cross-section	Length of Terrain cross-section (km)	Slope parts	The average length of the slope part (km)
Al-Sharhani watershed			
Headwaters	2.664	31	0.085
Middle	7.203	83	0.086
Mouth	8.927	103	0.086
Longitudinal section	18.675	215	0.086
Abu-Ghraibat watershed			
Headwaters	18.803	216	0.087
Middle	12.365	143	0.086
Mouth	10.728	132	0.081
Longitudinal section	41.779	475	0.087
Al-Shakak watershed			
Headwaters	4.214	49	0.086
Middle	9.140	103	0.088
Mouth	5.313	61	0.087
Longitudinal section	18.525	209	0.088

Geodiversity refers to the variety of natural geological elements, including rocks, minerals, and fossils, as well as geomorphological features, such as landforms, landscapes, and topographical characteristics, along with soil properties and their associated systems and processes. (Quesada-Román et al., 2022) This definition has been expanded to encompass lithological, tectonic, geomorphological, soil, hydrological, and topographical components, as well as the physical processes occurring on both terrestrial and aquatic surfaces. This comprehensive approach has facilitated categorizing rocks, landforms, and soils based on their distinctiveness and representativeness.

The variation in watersheds within their areas is due to the influence of a group of overlapping factors, including the type of rocks, tectonic activities, climate, slope, natural vegetation, and time. Values less than 1% naturally move away from

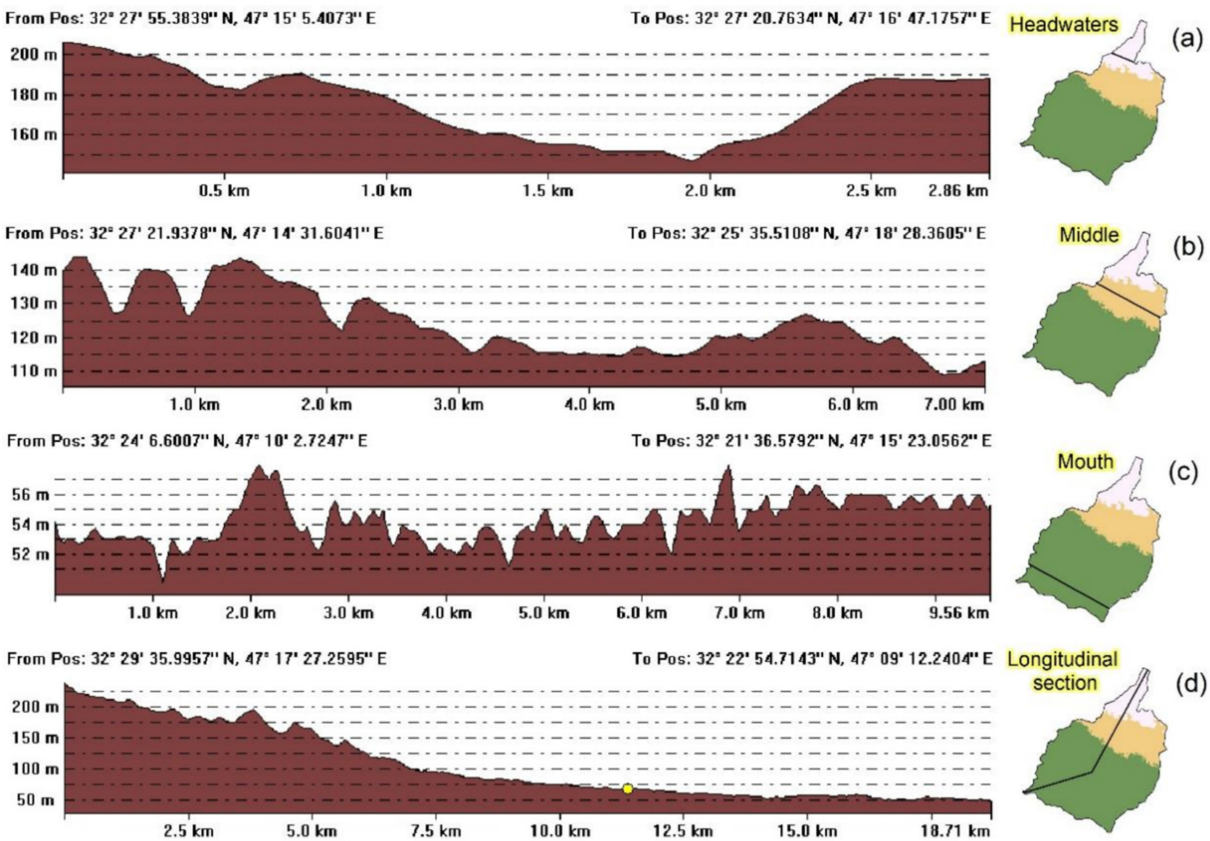

Fig. 15. Terrain cross-sections of the Al-Sharhani watershed.

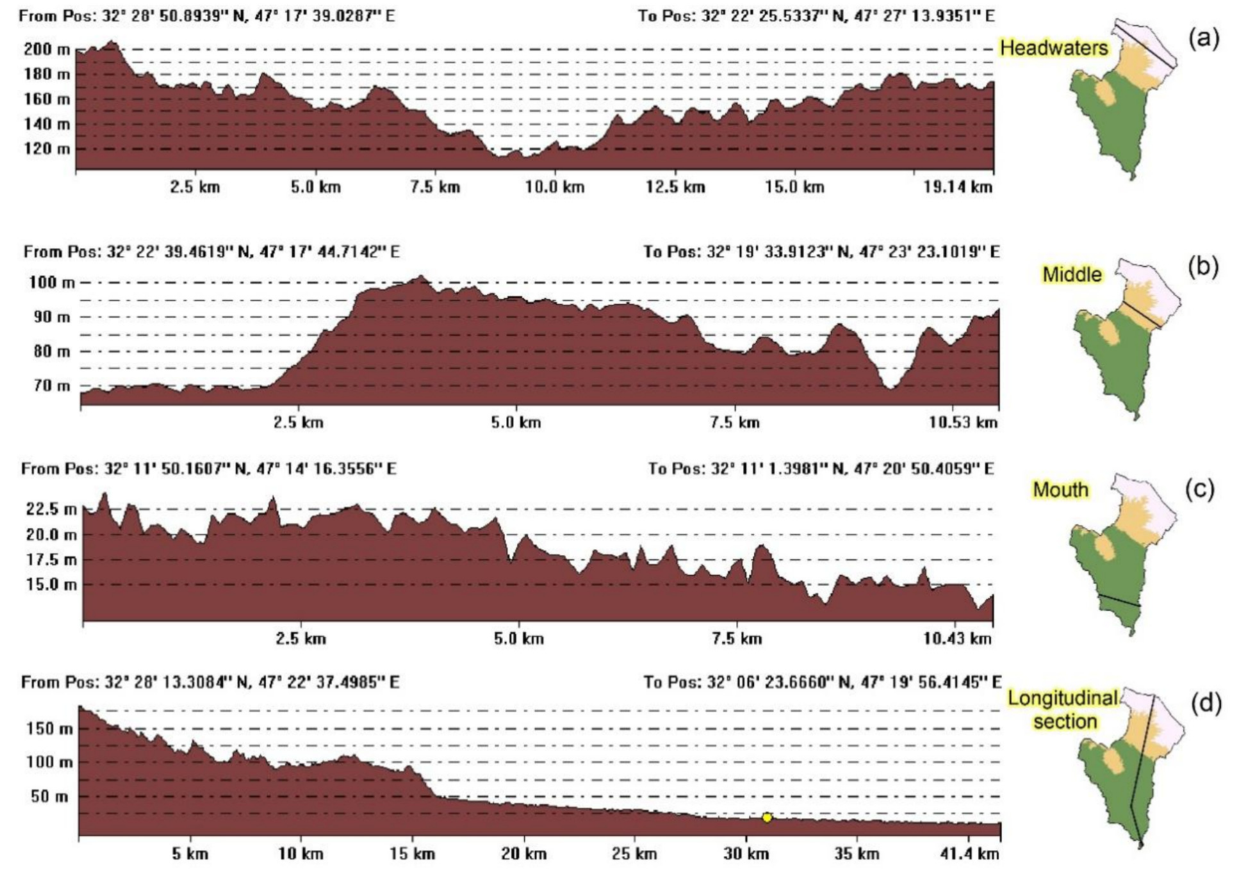

Fig. 16. Terrain cross-sections of Abu-Ghraibat watershed.

circularity and closer to elongation and vice versa. High values in some watersheds indicate that they are approaching a circular shape, resulting from an increase in the amount of rain and an increase in sediment yield. Additionally, water reaches the estuary quickly. This rapid delivery, combined with high drainage density, intensifies flooding and erosion, which can expand the channel network within the watershed. The low elongation ratio in some watershed sub-watersheds is due to faults extending along the watershed and the presence of solid rocks on both sides, which impede lateral erosion processes and hinder the widening of the watershed. The variation in the relief ratio values (R_h) is due to the variation in watershed areas. Watersheds with large areas have a lower relief ratio and vice versa. In addition to the effect of rock quality, watersheds with widespread hard rocks have a higher relief ratio, as these rocks are resistant to water erosion processes. Roughness values (R_n) vary during the stages of the geomorphological cycle referred to by Davies 1927. Roughness values decrease at the beginning of the cycle and then gradually increase until they reach a maximum at the onset of maturity of the geomorphological cycle, after which they decrease again in the ageing stage and at the end of the erosional cycle. Most watersheds are categorized as having a medium texture ratio (T) due to their weak, sandy, and dolomitic rock compositions, which are resistant to erosional processes. In addition, most of these watersheds are in the advanced stage of the erosion cycle, characterized by a flattening of the land. As for sub-watersheds, most of them fall into the category of coarse texture for the same reasons above. The variation in stream lengths is naturally due to variations in watershed areas, the degree of slope, and variations in rock hardness.

The slope category values indicate that the study area encompasses extensive regions of low-slope terrain, with limited areas exhibiting a steep slope. Figs. 13 and 14 demonstrate that most lands with elevated slope values are concentrated in the northern regions of the study area, specifically situated in the headwaters of the watersheds. The steep inclines in the watershed's upstream region align with its geomorphological phase, as these areas inherently undergo an initial stage of the geomorphological cycle defined by Davies in 1936. This stage remains in the geomorphological development phase, and as time progresses, it will undergo various erosion processes that erode its rocks, ultimately transforming it into a plain area. The slope director values demonstrate that the slope orientations align with the overall gradient of the study area's surface. The alignment of the slopes with the river drainage network, along with the courses of the streams, facilitates extensive erosion and shapes the overall orientation of the slopes through various geomorphological processes. The augmentation of slope segments in specific terrain cross-sections of the study area's watersheds is attributed to the water erosion

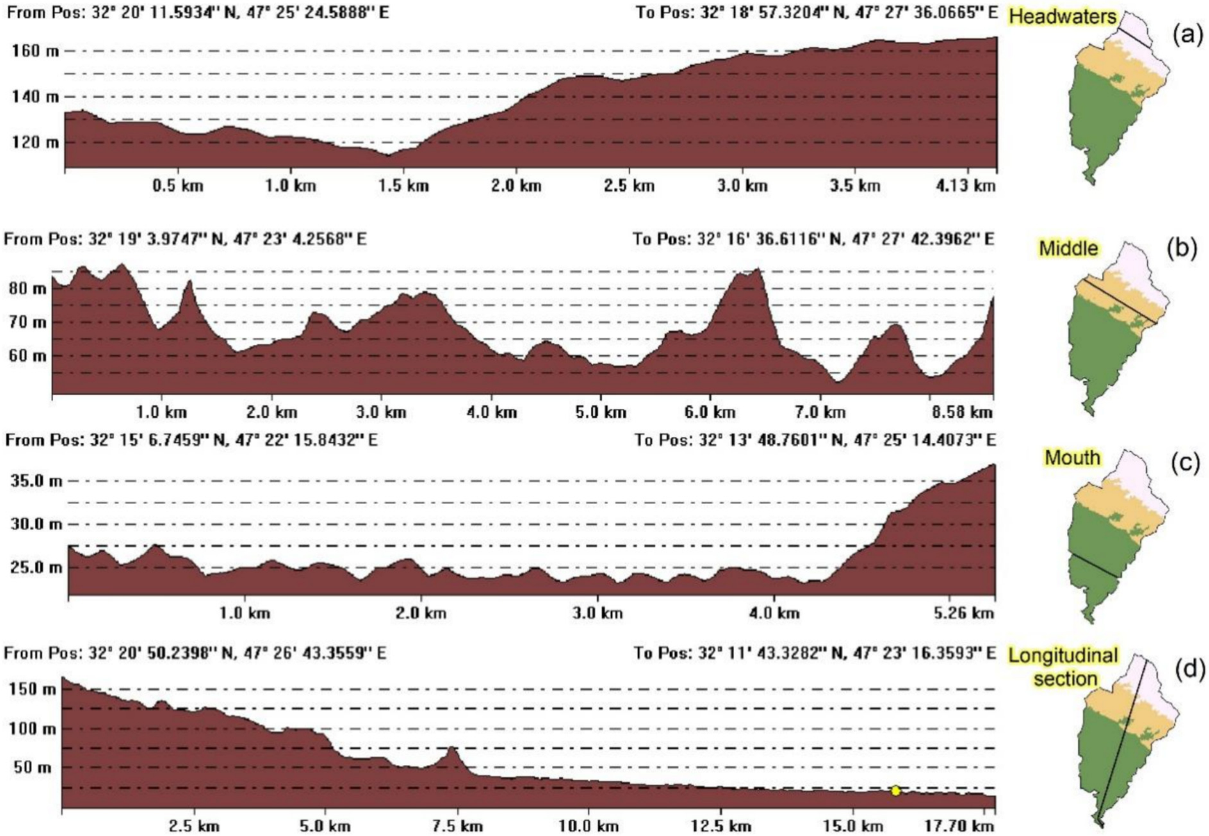

Fig. 17. Terrain cross-sections of the Al-Shakak watershed.

processes to which they are subjected, particularly since these regions are in the initial phase of the geomorphological cycle. The variation in stream orders between watersheds is directly proportional to the area of each watershed. A larger watershed area correlates with an increased number of streams.

Geotourism highlights some aspects of the Earth's geological and geomorphological heritage, which can either augment or diminish the significance of geoheritage. Once geoheritage is recognized and valued, the imperative for geoconservation arises. The geoconservation community must prioritize geographic heritage preservation within protected areas, enhancing its visibility on local, national, and international platforms concerning nature conservation, sustainable development, and human well-being (Pérez-Umaña, Quesada-Román, & Zangmo Tefogoum, 2020).

5. Conclusions

The study area comprises dome-shaped hills with steep slopes, created following the removal of soft rock and geological formations from the Tertiary period. Fault scarps, fissures in the Earth's crust, are prevalent in the eastern regions of Al-Zubaidat. Valleys and badlands are formed through precipitation and flowing water erosion, whereas alluvial plains, fans, floodplains, meanders, and dunes occupy extensive regions. Dunes are created by a deposit consisting predominantly of sand and silt. The Al-Zubaidat region has three primary watersheds (Al-Sharhani, Abu-Ghraibat, and Al-Shakak) and twelve sub-watersheds. The largest is Abu-Ghraibat, while the most extensive sub-watershed is SW6. The watershed perimeter correlates with the circulating ratio, form factor, and elongation ratio, where more significant perimeters signify larger areas. Comprehending these factors can facilitate the prediction of watershed characteristics and potential alterations. The watersheds of the study area are classified into five slope categories, each defined by slope characteristics corresponding to its geomorphological stage. The maximum value is located in the Abu-Ghraibat watershed, whereas the minimum is in the Al-Sharhani watershed. The sub-watersheds exhibit varying slope classifications, with SW6 possessing the steepest slopes and SW8 the gentlest. The study area encompasses extensive regions of low-slope terrain, interspersed with smaller areas exhibiting significant slopes. Most regions with elevated slope values are located in the northern sections of the study area, particularly in the headwaters region. Slope gradients vary across the watersheds, with the Abu-Ghraibat watershed having the steepest gradient and the Al-Sharhani watershed the gentlest.

CRediT authorship contribution statement

Bashar F. Maaroof: Writing – original draft, Visualization, Validation, Supervision, Methodology, Investigation, Formal analysis, Data curation, Conceptualization. **Hashim H. Kareem:** Writing – review & editing, Validation, Resources, Project administration. **Ban A.L.- Hasani:** Writing – review & editing, Supervision, Formal analysis, Data curation. **Iacopo Carnacina:** Validation, Software, Methodology, Investigation. **Mawada Abdellatif:** Supervision, Methodology, Formal analysis. **Nadhir Al-Ansari:** Validation, Methodology, Formal analysis. **Rayan G. Thannoun:** Methodology, Formal analysis, Data curation. **Jaffar H. Al-Zubaydi:** Validation, Methodology, Data curation. **Varoujan K. Sissakian:** Validation, Methodology, Data curation. **Mohammed A. Al-Musawi:** Validation, Methodology, Data curation. **Raheem H. Al-Abdan:** Validation, Methodology, Data curation. **Jaafar Jotheri:** Validation, Methodology, Data curation. **Hussain M. Hussain:** Validation, Methodology, Data curation. **Manal Sh. Al-Kubaisi:** Validation, Methodology, Data curation. **Ahmed M. Hashoosh:** Validation, Methodology, Data curation.

Declaration of competing interest

The authors declare that they have no known competing financial interests or personal relationships that could have appeared to influence the work reported in this paper.

Acknowledgements

The authors thank the Department of Geography at the University of Misan in Iraq, the Civil Engineering and Built Environment Department at Liverpool John Moores University, the Iraqi Geological Survey, and the Babylon Center for Civilization and Historical Studies at the University of Babylon for their scientific support during the study.

References

Abboud, I. A., & Nofal, R. A. (2017). Morphometric analysis of Wadi Khumal basin, western coast of Saudi Arabia, using remote sensing and GIS techniques. *Journal of African Earth Sciences*, *126*, 58–74. https://doi.org/10.1016/j.jafrearsci.2016.11.024.
Agha, O. M. A. M., & Şarlak, N. (2016). Spatial and temporal patterns of climate variables in Iraq. *Arabian Journal of Geosciences*, *9*(4), 302. https://doi.org/10.1007/s12517-016-2324-y.
Alexandrowicz, Z., & Margielewski, W. (2010). Impact of mass movements on geo- and biodiversity in the polish outer (flysch) Carpathians. *Geomorphology*, *123*(3–4), 290–304. https://doi.org/10.1016/j.geomorph.2010.07.020.
Al-Hasani, B., Abdellatif, M., Carnacina, I., Harris, C., Al-Quraishi, A., Maaroof, B. F., & Zubaidi, S. L. (2024b). Integrated geospatial approach for adaptive rainwater harvesting site selection under the impact of climate change. *Stochastic Environmental Research and Risk Assessment*, *38*(3), 1009–1033. https://doi.org/10.1007/s00477-023-02611-0.
Al-Hasani, B., Abdellatif, M., Carnacina, I., Harris, C., Al-Quraishi, A. M. F., & Maaroof, B. F. (2024a). Assessing climate change impacts on rainfall-runoff in northern Iraq: A case study of Kirkuk governorate, a semi-arid region. In A. Al-Quraishi, A. Negm, & B. Benzougagh (Eds.), *Climate change and environmental degradation in the MENA region* (pp. 93–111). Cham: Springer. https://doi.org/10.1007/698_2024_1154.
Al-Hasani, B., Abdellatif, M., Carnacina, I., Harris, C., Maaroof, B. F., & Zubaidi, S. L. (2025). Rainwater harvesting site assessment using geospatial Technologies in a Semi-Arid Region: Toward water sustainability. *Water*, *17*(15), 2317. https://doi.org/10.3390/w17152317.
Al-Janabi, K. Z., Jawad Ali, A., Al-Taie, F. H., & Jack, F. J. (1988). Origin and nature of sand dunes in the alluvial plain of Southern Iraq. *Journal of Arid Environments*, *14*(1), 27–34. https://doi.org/10.1016/s0140-1963(18)31093-0.
Al-Jiburi, H. (2005). *Hydrogeological and hydrochemical study of Al-Amara quadrangle*. State Company of Geological Survey and Mining.
Al-Jiburi, H. K., & Al-Basrawi, N. H. (2011). Hydrogeology of the Mesopotamia plain. *Iraqi Bulletin of Geology and Mining*, *5*, 83–103.
Al-Salih, S., & Al-Kubaisi, Q. (2016). Hydrochemical assessment of water resouces in Al-Teeb area, ne Maissan governate, South Iraq. *Iraqi Bulletin of Geology and Mining*, *12*(2), 1–12.
Arefin, R., Mohir, M. M. I., & Alam, J. (2020). Watershed prioritization for soil and water conservation aspect using GIS and remote sensing: PCA-based approach at northern elevated tract Bangladesh. *Applied Water Science*, *10*(4), 91. https://doi.org/10.1007/s13201-020-1176-5.
Carrión-Mero, P., Montalván-Burbano, N., Herrera-Narváez, G., & Morante-Carballo, F. (2021). Geodiversity and mining towards the development of geotourism: A global perspective. *International Journal of Design & Nature and Ecodynamics*, *16*(2), 191–201. https://doi.org/10.18280/ijdne.160209.
Crofts, R. (2019). Linking geoconservation with biodiversity conservation in protected areas. *In International Journal of Geoheritage and Parks*, *7*(4), 211–217. https://doi.org/10.1016/j.ijgeop.2019.12.002.
Dinagara Pandi, P., Thena, T., Nirmal, B., Aswathy, M. R., Saravanan, K., & Mohan, K. (2017). Morphometric analyses of Neyyar River basin, southern Kerala, India. *Geology, Ecology, and Landscapes*, *1*(4), 249–256. https://doi.org/10.1080/24749508.2017.1389494.
Diniz, M. T. M., de Araújo, I. G. D., & das Chagas, M. D. (2022). Comparative study of quantitative assessment of the geomorphological heritage of the coastal zone of Icapuí - Ceará, Brazil. *International Journal of Geoheritage and Parks*, *10*(1), 124–142. https://doi.org/10.1016/j.ijgeop.2022.02.006.
Fenta, A. A., Yasuda, H., Shimizu, K., Haregeweyn, N., & Woldearegay, K. (2017). Quantitative analysis and implications of drainage morphometry of the Agula watershed in the semi-arid Northern Ethiopia. *Applied Water Science*, *7*(7), 3825–3840. https://doi.org/10.1007/s13201-017-0534-4.
Fouad, S. F., & Sissakian, V. K. (2011). Tectonic and structural evolution of the Mesopotamia plain. *Iraqi Bulletin of Geology and Mining*, *4*, 33–46.
Fouad, S. F. A. (2010). Tectonic and structural evolution of the Mesopotamia Foredeep, Iraq. *Iraqi Bulletin of Geology and Mining*, *6*(2), 41–53.
Fouad, S. F. A. (2015). Tectonic map of Iraq, scale 1:1,000,000. *Iraqi Bulletin of Geology and Mining*, *11*(1), 1–7.
Gałaś, A., Paulo, A., Gaidzik, K., Zavala, B., Kalicki, T., Churata, D., Gałaś, S., & Mariño, J. (2018). Geosites and geotouristic attractions proposed for the project Geopark Colca and volcanoes of Andagua Peru. *Geoheritage*, *10*(4), 707–729. https://doi.org/10.1007/s12371-018-0307-y.
Gordon, J. E. (2019). Geoconservation principles and protected area management. *International Journal of Geoheritage and Parks*, *7*(4), 199–210. https://doi.org/10.1016/j.ijgeop.2019.12.005.
Gordon, J. E., Crofts, R., Díaz-Martínez, E., & Woo, K. S. (2018). Enhancing the role of geoconservation in protected area management and nature conservation. *Geoheritage*, *10*(2), 191–203. https://doi.org/10.1007/s12371-017-0240-5.
Gordon, J. E., Crofts, R., Gray, M., & Tormey, D. (2021). Including geoconservation in the management of protected and conserved areas matters for all of nature and people. *International Journal of Geoheritage and Parks*, *9*(3), 323–334. https://doi.org/10.1016/j.ijgeop.2021.05.003.
Gray, M., Gordon, J. E., & Brown, E. J. (2013). Geodiversity and the ecosystem approach: The contribution of geoscience in delivering integrated environmental management. *Proceedings of the Geologists' Association*, *124*(4), 659–673. https://doi.org/10.1016/j.pgeola.2013.01.003.
Henriques, M. H., & Brilha, J. (2017). UNESCO global Geoparks: A strategy towards global understanding and sustainability. *Episodes*, *40*(4), 349–355. https://doi.org/10.18814/epiiugs/2017/v40i4/017036.

Hjort, J., Heikkinen, R. K., & Luoto, M. (2012). Inclusion of explicit measures of geodiversity improve biodiversity models in a boreal landscape. *Biodiversity and Conservation*, *21*(13), 3487–3506. https://doi.org/10.1007/s10531-012-0376-1.
Horton, R. E. (1945). Erosional development of streams and their drainage basins; hydrophysical approach to quantitative morphology. *Bulletin of the Geological Society of America*, *56*(3), 275–370. https://doi.org/10.1130/0016-7606(1945)56[275:EDOSAT]2.0.CO;2.
Kubalíková, L. (2020). Cultural ecosystem services of geodiversity: A case study from Stranska skala (Brno, Czech Republic). *Land*, *9*(4), 105. https://doi.org/10.3390/land9040105.
Maaroof, B., Kareem, H., Al-Zubaydi, J., Thannoun, R., Al-Kubaisi, M., Hasani, A. L., ... Carnacina, I. (2025). Classifying fluvial landforms using geospatial modeling in Al-Ashaali watershed, Iraqi Southern Desert. *Bulletin of the Iraq Natural History Museum*, *18*(3), 739–763. https://doi.org/10.26842/binhm.7.2025.18.3.0739.
Maaroof, B., Omran, M., Al-Qaim, F., Salman, J., Hussain, B., Abdellatif, M., ... Hussein, W. (2023). Environmental assessment of Al-Hillah River pollution at Babil Governorate (Iraq). *Journal of the Geographical Institute Jovan Cvijic, SASA*, *73*(1), 1–16. https://doi.org/10.2298/IJGI2301001M.
Maaroof, B. F. (2022a). Geomorphological assessment using geoinformatics applications of the sloping system of Al-Ashaali Drainage Basin at Iraqi Southern Desert. *Iraqi National Journal of Earth Science*, *22*(1), 38–54. https://doi.org/10.33899/earth.2022.133146.1009.
Maaroof, B. F. (2022b). Geomorphometric assessment of the river drainage network at Al-Shakak Basin (Iraq). *Journal of the Geographical Institute Jovan Cvijic SASA*, *72*(1), 1–13. https://doi.org/10.2298/IJGI2201001M.
Maaroof, B. F. (2024). Quantitative analysis using geospatial modeling of Al-Rahimaw watershed's shape properties in the Iraqi Southern Desert. *Bulletin of the Iraq Natural History Museum*, *18*(2), 277–295. https://doi.org/10.26842/binhm.7.2024.18.2.0277.
Maaroof, B. F. (2025). Fluvial landforms classification using geospatial modeling of Al-Jazeera eastern region at Misan Governorate, Iraq. *Iraqi National Journal of Earth Science*, *25*(2), 199–218. https://doi.org/10.33899/earth.2024.146564.1228.
Maaroof, B. F., Al-Abdan, R. H., & Kareem, H. H. (2021). Geographical assessment of natural resources at Abu-Hadair Drainage Basin in Al-Salman Desert. *Indian Journal of Ecology*, *48*(3), 797–802. Retrieved from https://www.indianjournals.com/ijor.aspx?target=ijor:ije1&volume=47&issue=3&article=007.
Maaroof, B. F., Al-Musawi, M. A., Kareem, H. H., Al-Abdan, R. H., Obaid, H. S., Al-Hasani, B., ... Carnacina, I. (2023). Geographical assessment of the natural environment at Al-Huwaizah Marsh, Eastern of Misan Governorate, Iraq. *Misan Journal of Academic Studies*, *26*(22), 293–310. https://doi.org/10.54633/2333-022-046-019.
Maaroof, B. F., & Kareem, H. H. (2020). Water erosion of the slopes of Tayyar drainage basin in the desert of Muthanna in Southern Iraq. *Indian Journal Of Ecology*, *47*(3), 638–644. Retrieved from https://www.indianjournals.com/ijor.aspx?target=ijor:ije1&volume=47&issue=3&article=007.
Maaroof, B. F., & Kareem, H. H. (2022). Geomorphometric analysis of Al -Teeb River meanders between Al-Sharhani Basin and Al-Sanaf Marsh, eastern of Misan Governorate, Iraq. *Misan Journal of Academic Studies*, *21*(42), 441–455. https://doi.org/10.54633/2333-021-042-033.
Maaroof, B. F., & Kareem, H. H. (2023). Geomorphological analysis of chemical weathering features in Al-Band Hills area, eastern of Misan governorate, Iraq. *Iraqi National Journal of Earth Science*, *23*(1), 67–84. https://doi.org/10.33899/earth.2023.137382.1034.
Mucivuna, V. C., Garcia, M. G. M., Reynard, E., & Rosa, P. A. S. (2022). Integrating geoheritage into the management of protected areas: A case study of the Itatiaia National Park, Brazil. *International Journal of Geoheritage and Parks*, *10*(2), 252–272. https://doi.org/10.1016/j.ijgeop.2022.04.004.
Najwer, A., Jankowski, P., Niesterowicz, J., & Zwoliński, Z. (2022). Geodiversity assessment with global and local spatial multicriteria analysis. *International Journal of Applied Earth Observation and Geoinformation*, *107*, Article 102665. https://doi.org/10.1016/j.jag.2021.102665.
Pardo-Igúzquiza, E., & Dowd, P. A. (2021). The mapping of closed depressions and its contribution to the geodiversity inventory. *International Journal of Geoheritage and Parks*, *9*(4), 480–495. https://doi.org/10.1016/j.ijgeop.2021.11.007.
Pereira, D. I., Pereira, P., Brilha, J., & Santos, L. (2013). Geodiversity assessment of Paraná state (Brazil): An innovative approach. *Environmental Management*, *52*(3), 541–552. https://doi.org/10.1007/s00267-013-0100-2.
Pereira, L. S., & da Silva Farias, T. (2020). Assessing the cultural values of the geodiversity in a Brazilian city: The historical center of João Pessoa (Paraíba, NE Brazil), Mata da Aldeia chart. *International Journal of Geoheritage and Parks*, *8*(1), 59–73. https://doi.org/10.1016/j.ijgeop.2020.03.002.
Pérez-Umaña, D., Quesada-Román, A., & Zangmo Tefogoum, G. (2020). Geomorphological heritage inventory of Irazú volcano, Costa Rica. *International Journal of Geoheritage and Parks*, *8*(1), 31–47. https://doi.org/10.1016/j.ijgeop.2019.12.001.
Prasannakumar, V., Shiny, R., Geetha, N., & Vijith, H. (2011). Applicability of SRTM data for landform characterisation and geomorphometry: A comparison with contour-derived parameters. *International Journal of Digital Earth*, *4*(5), 387–401. https://doi.org/10.1080/17538947.2010.514010.
Quesada-Román, A., & Pérez-Umaña, D. (2020). State of the art of geodiversity, geoconservation, and geotourism in Costa Rica. *Geosciences*, *10*(6), 1–17. https://doi.org/10.3390/geosciences10060211.
Quesada-Román, A., Torres-Bernhard, L., Ruiz-álvarez, M. A., Rodríguez-Maradiaga, M., Velázquez-Espinoza, G., Espinosa-Vega, C., ... Rodríguez-Bolaños, H. (2022). Geodiversity, geoconservation, and geotourism in Central America. *Land*, *11*(1), 48. https://doi.org/10.3390/land11010048.
Quesada-Román, A., Zangmo, G. T., & Pérez-Umaña, D. (2020). Geomorphosite comparative analysis in Costa Rica and Cameroon volcanoes. *Geoheritage*, *12*(4), 90. https://doi.org/10.1007/s12371-020-00515-x.
Quesada-Valverde, M. E., & Quesada-Román, A. (2023). Worldwide trends in methods and resources promoting geoconservation, geotourism, and geoheritage. *Geosciences*, *13*(2), 39. https://doi.org/10.3390/geosciences13020039.
Resmi, M. R., Babeesh, C., & Achyuthan, H. (2019). Quantitative analysis of the drainage and morphometric characteristics of the Palar River basin, southern peninsular India; using bAd calculator (bearing azimuth and drainage) and GIS. *Geology, Ecology, and Landscapes*, *3*(4), 295–307. https://doi.org/10.1080/24749508.2018.1563750.
Schumm, S. A. (1956). Evolution of drainage systems and slopes in Balands at Perthamboy, New Jersey. *Geological Society of America Bulletin*, *67*(6), 597–646. https://doi.org/10.1130/0016-7606(1956)67.
Schumm, S. A. (1963). Sinuosity of alluvial rivers on the Great Plains. *Geological Society of America Bulletin*, *74*(9), 1089–1100.
Sissakian, V. K., & Fouad, S. F. A. (2015). Geological map of Iraq, scale 1:1,000,000. *Iraqi Bulletin of Geology and Mining*, *11*(1), 9–16.
Sissakian, V. K., Jab'bar, M. F. A., & Jabbar, M. F. A. (2014). Classification of the alluvial fans in Iraq. *Iraqi Bulletin of Geology and Mining*, *10*(3), 43–67.
Smith, K. G. (1950). Standards for grading texture of erosional topography. *American Journal of Science*, *248*, 655–668.
Strahler, A. N. (1954). Statistical analysis in geomorphic research. *The Journal of Geology*, *62*(1), 1–25. https://doi.org/10.1086/626131.
Strahler, A. N. (1957). Quantitative analysis of watershed geomorphology. *Eos, Transactions American Geophysical Union*, *38*(6), 913–920. https://doi.org/10.1029/TR038i006p00913.
Umrikar, B. N. (2017). Morphometric analysis of Andhale watershed, Taluka Mulshi, District Pune, India. *Applied Water Science*, *7*(5), 2231–2243. https://doi.org/10.1007/s13201-016-0390-7.
Yacoub, S. Y. (2011a). Geomorphology of the Mesopotamia plain. *Iraqi Bulletin of Geology and Mining*, *7*(4), 7–32.
Yacoub, S. Y. (2011b). Stratigraphy of the Mesopotamia plain. *Iraqi Bulletin of Geology and Mining*, *7*(4), 74–82.
Yacoub, S. Y. (2010). Geomorphology of the Mesopotamian plain: A critical review. *Journal of Earth Sciences and Geotechnical Engineering*, *10*(4), 1–25.
Zarnetske, P. L., Read, Q. D., Record, S., Gaddis, K. D., Pau, S., Hobi, M. L., ... Finley, A. O. (2019). Towards connecting biodiversity and geodiversity across scales with satellite remote sensing. *Global Ecology and Biogeography*, *28*(5), 548–556. https://doi.org/10.1111/geb.12887.